

DELFT UNIVERSITY OF TECHNOLOGY

DEPARTMENT OF AEROSPACE ENGINEERING

Report LR-281

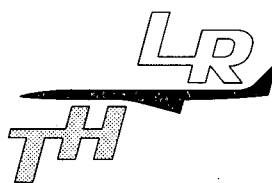
**AERODYNAMIC CHARACTERISTICS OF A CURVED
PLATE AIRFOIL SECTION AT REYNOLDS NUMBERS
60.000 AND 100.000 AND ANGLES OF ATTACK
FROM -10 TO +90 DEGREES**

by

A. Bruining

DELFT - THE NETHERLANDS

May 1979



DELFT UNIVERSITY OF TECHNOLOGY

DEPARTMENT OF AEROSPACE ENGINEERING

Report LR-281

**AERODYNAMIC CHARACTERISTICS OF A CURVED
PLATE AIRFOIL SECTION AT REYNOLDS NUMBERS
60.000 AND 100.000 AND ANGLES OF ATTACK
FROM -10 TO +90 DEGREES**

by

A. Bruining

DELFT - THE NETHERLANDS

May 1979

SUMMARY

This report contains the results of lift and drag measurements on a two-dimension airfoil consisting of a circular arc steel plate with 10% camber. The measurements included the determinations of the influence of a turbular spar (diameter 6.67% chord) mounted at different positions around the blade (at the leading-edge and at 25% and 50% chord on upper and lower surface). The tests were performed at chord Reynoldsnumbers 60.000, 100.000, and some 200.000; the angle of attack was varied between -10 and +90 degrees.

The results show that a spar position on the low pressure side of the blade leads to a best lift-drag ratio of not more than about 5. The other spar positions produce lift-drag ratio of the order of 20.

The measurements were performed in the low-speed windtunnel of the Department of Aerospace Engineering at the Delft University of Technology.

CONTENTS

	page
Summary	1
Symbols	3
1. Introduction	5
2. Apparatus, Tests, Methods	6
2.1. Windtunnel	6
2.2. Model	6
2.3. Instrumentation	6
2.4. Tests	7
2.5. Corrections for tunnel blockage	7
3. Results	8
4. Conclusions	9
5. References	10
Tables	
Figures	

SYMBOLS

A	$= \pi R^2$ area rotor	m^2
c	airfoil chord	m
c_d	$= \frac{D}{\frac{1}{2} \rho U_m^2 c}$ section drag coefficient	
c_l	$= \frac{L}{\frac{1}{2} \rho U_m^2 c}$ section lift coefficient	
C_p	$= \frac{P}{\frac{1}{2} \rho U_m^3 A}$ power coefficient of windmill	
D	drag per unit span	N/m
L	lift per unit span	N/m
p_m	$= \frac{p_{w1} + p_{w2}}{2}$ effective free stream static pressure	N/m^2
p_{w1}	static pressure at tunnelwall, measured opposite the 25% chord position on the low pressure side, see fig. 2	N/m^2
p_{w2}	static pressure at tunnelwall, measured opposite the 25% chord position on the high pressure side, see fig. 2	N/m^2
$p_{t\infty}$	free stream total pressure	N/m^2
P	power	W
q_m	$= p_{t\infty} - p_m$ effective free stream dynamic pressure	N/m^2
R	radius rotor	
Re	$= \frac{U_m c}{\nu}$ Reynoldsnumber based on airfoil chord	
U_m	$= \sqrt{\frac{2q_m}{\rho}}$ effective free stream velocity	m/s
α	section angle of attack	degrees

λ ratio of tip speed of windmill rotor to windspeed

ν kinematic viscosity of air m^2/s

ρ air density kg/m^3

1. INTRODUCTION

A curved plate is an interesting airfoil for windmills, especially for the smaller slow running types, which do not need high quality airfoils. Manufacturing is easy and cheap for such simple blades.

In the Netherlands a small windmill of a certain type is used extensively for pumping water. This windmill has four blades consisting of curved metal plates. On the low pressure side of the blades a tube is mounted at the 25% chord position to fasten the blades to the horizontal axis.

From aerodynamic considerations it can be expected that this position of the tube is unfavourable. Therefore other positions of the tube on the blade and a blade without a tube have been investigated in the windtunnel to see how much improvement can be obtained.

During the starting phase of a windmill high angles of attack occur; therefore the measurements were carried out also for high angles of attack.

2. APPARATUS, TESTS, METHODS

2.1. Windtunnel

The present investigation was made in the low-speed, low-turbulence windtunnel of the Department of Aerospace Engineering at the Delft University of Technology. The test section of the tunnel has a closed octagonal cross-section, 1.80 m wide and 1.25 m high. At the speeds at which the tests have been performed the turbulence level is of the order of .02%.

2.2. Model

The two-dimensional model consisted of a curved steel plate with 10% camber. The model has a span of .75 m and a chordlength of .15 m. The model was mounted between two flat plates to eliminate the influence of the tunnelwall boundary layers. The rotation centre was located at 25% of the model chord line. A sketch of the model is shown in fig. 3; the test setup is shown in figs. 1 and 2.

The characteristics of the blade were determined with and without a tubular spar (diameter .01 m = 6.67% chord). This tube could be mounted with three screws at different positions around the blade, shown in table 1 and fig. 3.

2.3. Instrumentation

Forces were measured by a six component balance system connected to a PDP-8/L processor. A pitot-static tube (height .25 m) was placed on the floor of the test section 1.06 m ahead of the rotation centre of the airfoil and .36 m out of the vertical plane of symmetry. On each side-wall one static pressure hole was located opposite the 25% chord point (see fig. 1 and 2). The pressures were measured by a Mensor Quarts Manometer of the direct reading type.

2.4. Tests

The airfoil was tested at Reynoldsnumbers of 60.000, 100.000 and some configurations at 200.000 over an angle of attack range from -10 to +90 degrees. The PDP-8/L processor calculated directly the section lift coefficient and the section drag coefficient from the balance forces.

In ref. 3 the section drag coefficient for the clean model was determined with a wake rake, as indicated in figs. 1 and 2. For present purposes the differences in drag obtained from wake rake and balance force measurements are of minor importance.

Tests were made with a clean model and with the tube mounted at the locations mentioned in table 1.

2.5. Corrections for tunnel blockage

Due to the finite size of the windtunnel test section it is impossible to indicate a position where the free stream static pressure and -speed could be measured. Although the ratio of model chord (0.15 m) to tunnel width (1.80 m) was very small, the tunnel blockage due to the presence of the model could not be neglected because of the high angles of attack which have been used. A simple correction method was obtained by defining an "effective free stream static pressure" p_m as the mean of the two wall pressures p_{w1} and p_{w2} , measured at the side walls opposite the 25% chord position. No further corrections have been applied.

3. RESULTS

The section lift and drag characteristics of the blade for different tube positions and Reynoldsnumbers may be found in figs. 4 through 25. Several characteristic numbers have been collected in tables 2 and 3 for Reynoldsnumbers of 60.000 and 100.000 respectively.

The effect on the lift-drag ratio of moving the tube from the low pressure side to the high pressure side of the blade follows from figs. 26 and 27 for the Reynoldsnumbers of 60.000 and 100.000 respectively.

The influence of the Reynoldsnumbers is summarised in the figs. 28 and 29 respectively for the tube at the low and high pressure side.

4. CONCLUSIONS

1. If the tube is mounted on the low pressure side of the blade a $(c_l/c_d)_{\max}$ value from 3 till 5 is reached at angles of attack from 15 to 20 degrees. If the tube is placed on the leading edge or high pressure side the results are much better: $(c_l/c_d)_{\max}$ then reaches values from 16 to 20 at angles of attack from 5 to 8 degrees.
2. The exact position of the tube on either the high- or low pressure side of the blade is not very important: for example a slot of 0 or 4 mm between tube and blade makes very little difference. However the poorest results are obtained for the configuration with the tube on the low pressure side at the 25% chord position. This is just the position which is very often used in practice on small poldermills.
3. To show the effect of the tube position on the performance of a typical small windmill, the graphs in ref. 1 have been used to calculate the maximum power coefficient for a four-bladed windmill using the present results for c_l/c_d . It follows that moving the tube from the low pressure side to the leading-edge or the high pressure side results in an increase of the maximum power coefficient from about .25 to .4. Detailed results may be found in tables 2 and 3.
4. The c_l/c_d characteristics show a little improvement when the Reynoldsnumber is increased.
5. The angle of attack at stall varies between 16 and 20 degrees for the models with the tube on the high pressure side. For the other models stall occurs between 12 and 16 degrees. The airfoil with the tube at the leading edge has the largest stall angle of attack (at 16 degrees).

5. REFERENCES

1. Jansen, W.A.M. and Smulders, P.T. Rotor design for horizontal axis wind-mills, SWD 77-1, SWD P.O. Box 85 Amersfoort, The Netherlands, May 1977.
2. Dekker, Th.A.H. Performance characteristics of some sail- and steel-bladed windrotors. SWD 77-5, SWD P.O. Box 85 Amersfoort, The Netherlands, December 1977.
3. Volkers, D.F. Preliminary results of windtunnel measurements on some airfoil sections at Reynoldsnumbers between $.6 \cdot 10^5$ and $5.0 \cdot 10^5$. Memorandum M-276, Delft University of Technology, Department of Aerospace Engineering, The Netherlands, June 1977.
4. Beurskens, J., Honet, M., Varst, P. v.d. Wind Energy no. 3323. Eindhoven University of Technology, Eindhoven, The Netherlands, English edition 1977.



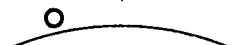

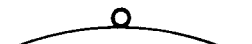
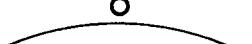
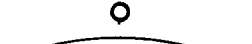
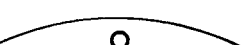

model configuration	model code	tube position
	-, -	no tube
	0, +0.0	leading edge high pressure side no slot
	25, -1.55	25% chord low pressure side slot 1.55 mm
	25, +1.55	25% chord high pressure side slot 1.55 mm
	50, -0.0	50% chord low pressure side no slot
	50, -1.55	50% chord low pressure side slot 1.55 mm
	50, -4.0	50% chord low pressure side slot 4.0 mm
	50, +4.0	50% chord high pressure side slot 4.0 mm
	50, +8.0	50% chord high pressure side slot 8.0 mm

Table 1: tube positions on curved plate.








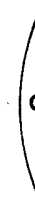

model configuration	model code	Conditions for (C_l/C_d) _{max}				Conditions for stall		C_{dmin}	Power coefficient and optimum λ for a 4 bladed windmill using this blade	
		α degrees	C_l/C_d	C_l	α_{stall} degrees	C_{lmax}	λ for C_{pmax}		C_{pmax}	
	-,-	8	15	1.4	12	1.48	.085	3	.39	
	0, +0.0	8	17	1.3	15	1.49	.062	3	.41	
	25, -1.55	19	3.4	1.25	22	1.32	.15	1	.20	
	25, +1.55	8	15.5	1.15	12	1.32	.05	3	.40	
	50, -0.0	15	5	1.25	16	1.29	.16	1.6	.26	
	50, -1.55	15	4.8	1.23	20	1.25	.165	1.6	.26	
	50, -4.0	15	4.9	1.2	19	1.26	.16	1.6	.26	
	50, +4.0	8	16.5	1.2	12	1.35	.062	3	.40	
	50, +8.0	6.5	17.5	1.23	12	1.42	.075	3.1	.41	

Table 2: Results for Reynoldsnumber 60.000.

model configuration	model code	Conditions for $(C_l/C_d)_{\max}$			Conditions for stall		$C_{d\min}$	Power coefficient and optimum λ for a 4 bladed windmill using this blade	
		α degrees	C_l/C_d	C_l	α_{stall} degrees	$C_{l\max}$		λ for $C_{p\max}$	$C_{p\max}$
	-,-	6	23	1.3	12	1.47	.06	3.6	.43
	0, +0.0	6	19	1.1	16	1.5	.06	3.2	.42
	25, -1.55	17	3.4	1.12	21	1.28	.16	1	.20
	25, +1.55	5	18	1.07	12.5	1.3	.06	3	.41
	50, -0.0	16	4.7	1.26	16	1.27	.16	1.6	.25
	50, -1.55	15	4.8	1.28	15	1.28	.17	1.6	.26
	50, -4.0	14	4.7	1.2	17	1.24	.17	1.6	.25
	50, +4.0	5	18	1.16	12	1.35	.07	3	.41
	50, +8.0	17.5	1.2	1.2	11	1.4	.07	3	.41

Table 3: Results for Reynoldsnumber 100.000.

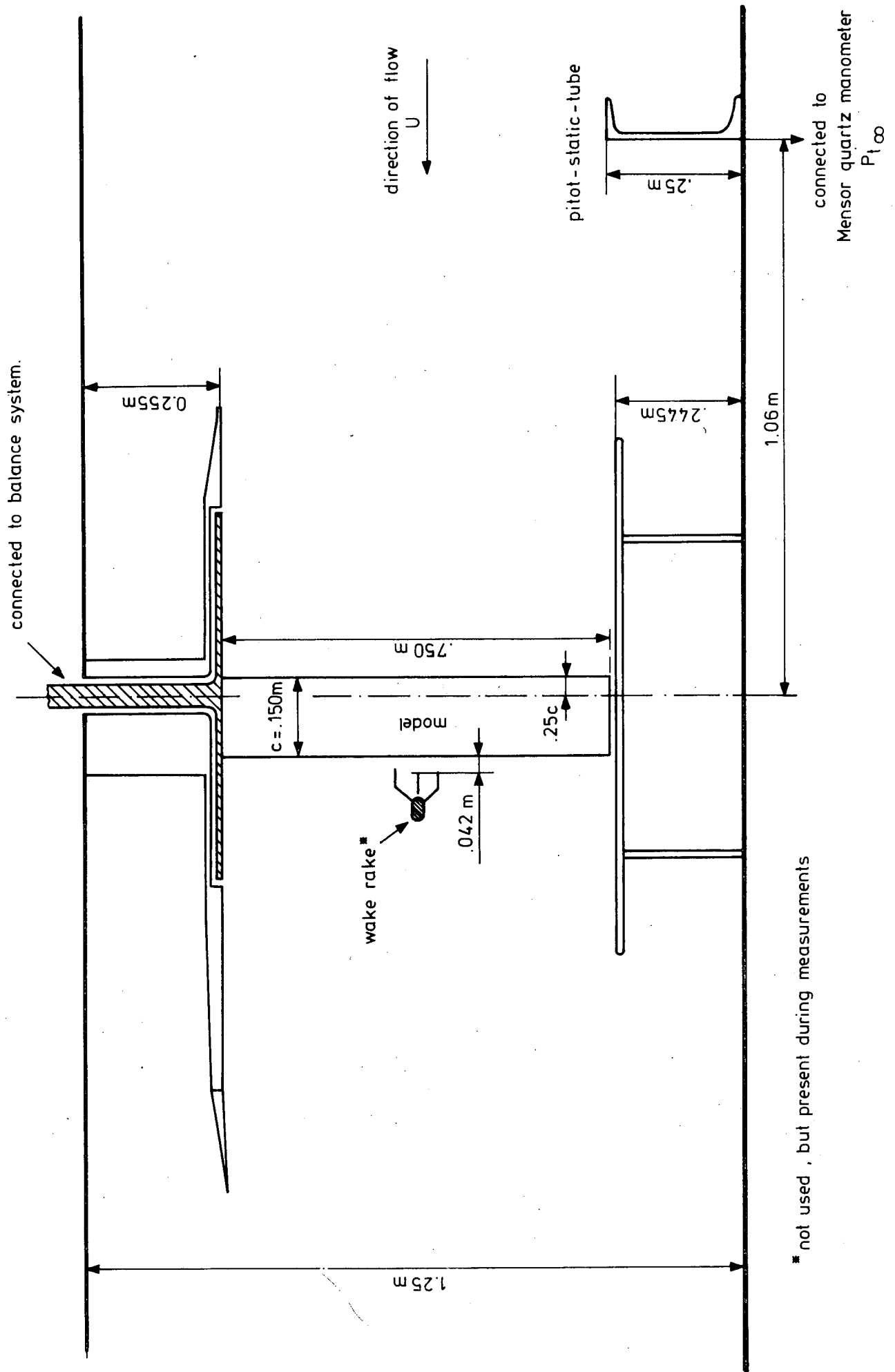


Fig. 1: Side-view of test section.

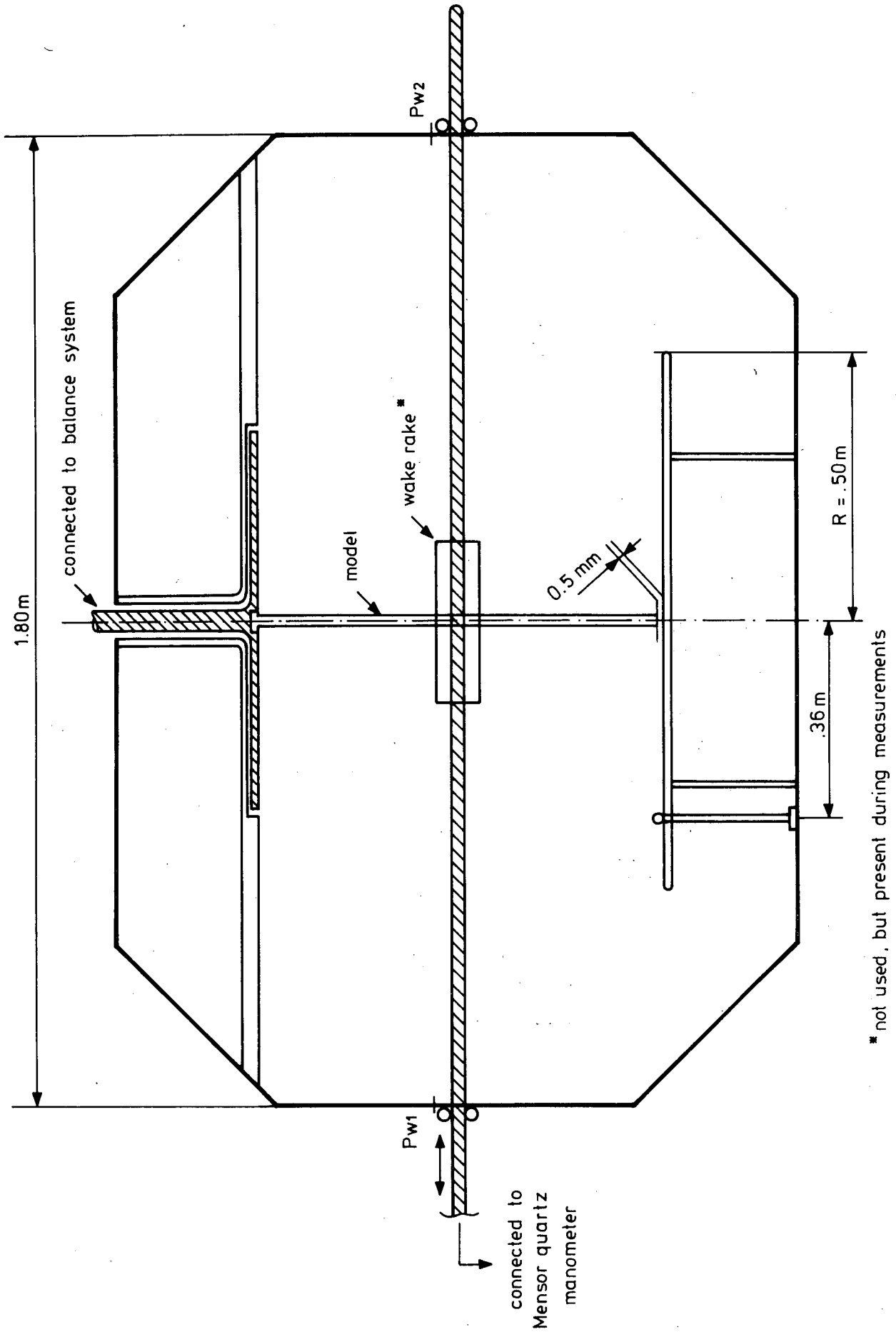


Fig. 2: Front-view of test section.

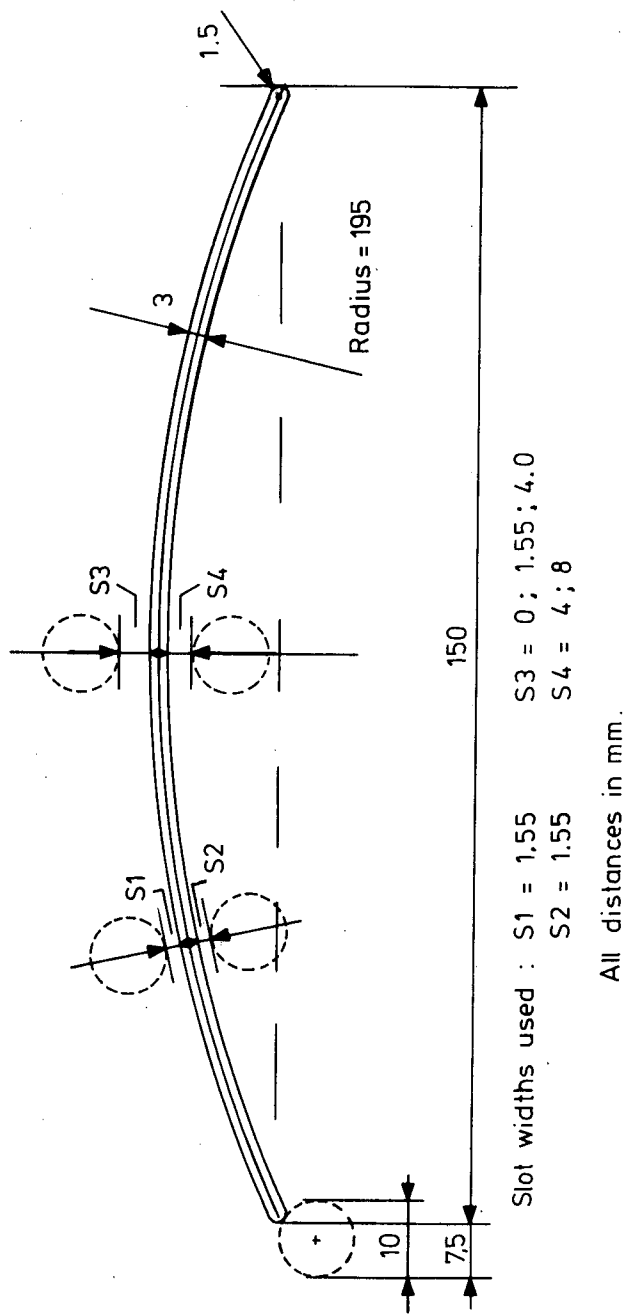


Fig. 3: Airfoil section employed for the investigation with indication of the positions of the tubular spar.

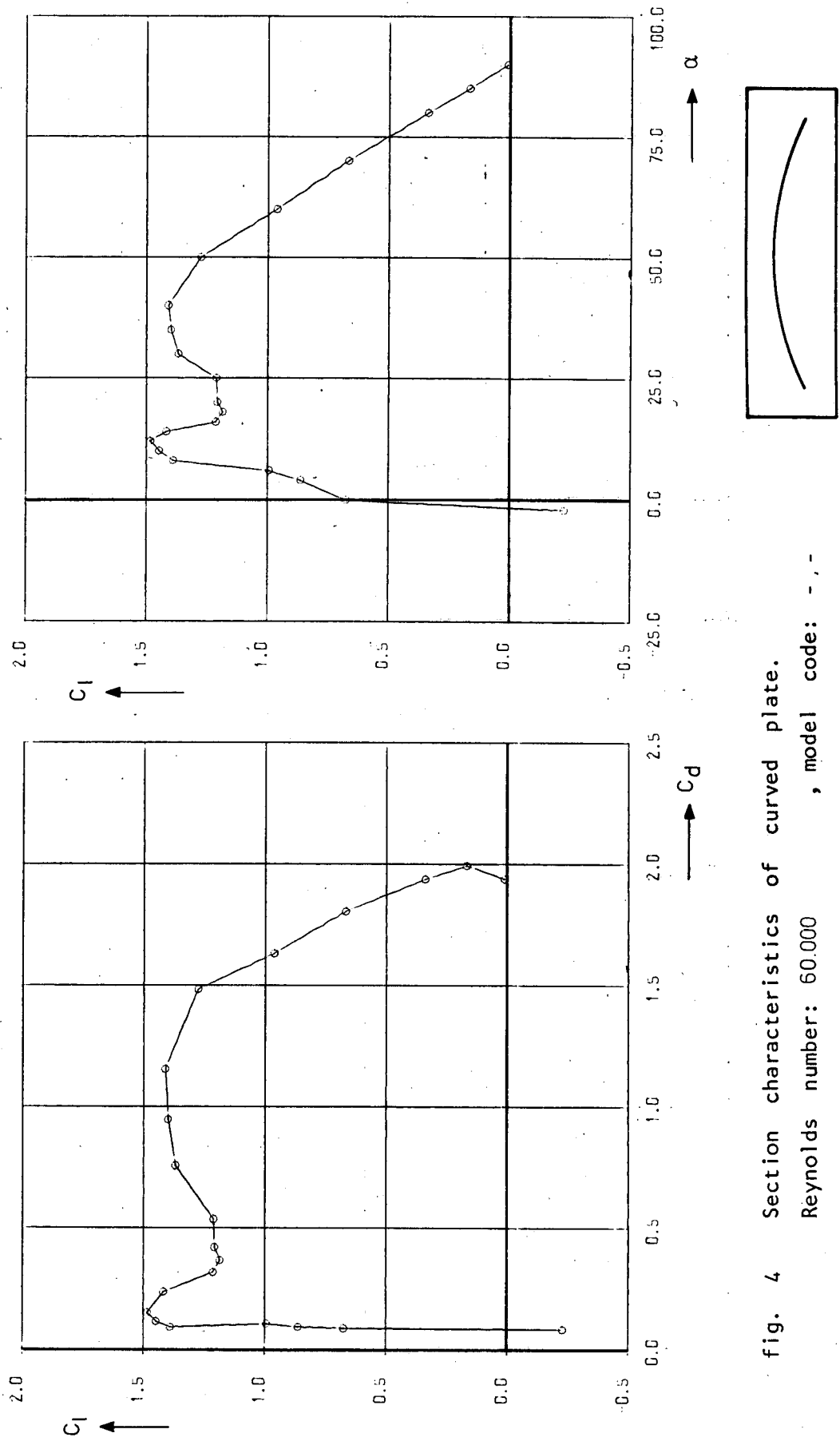
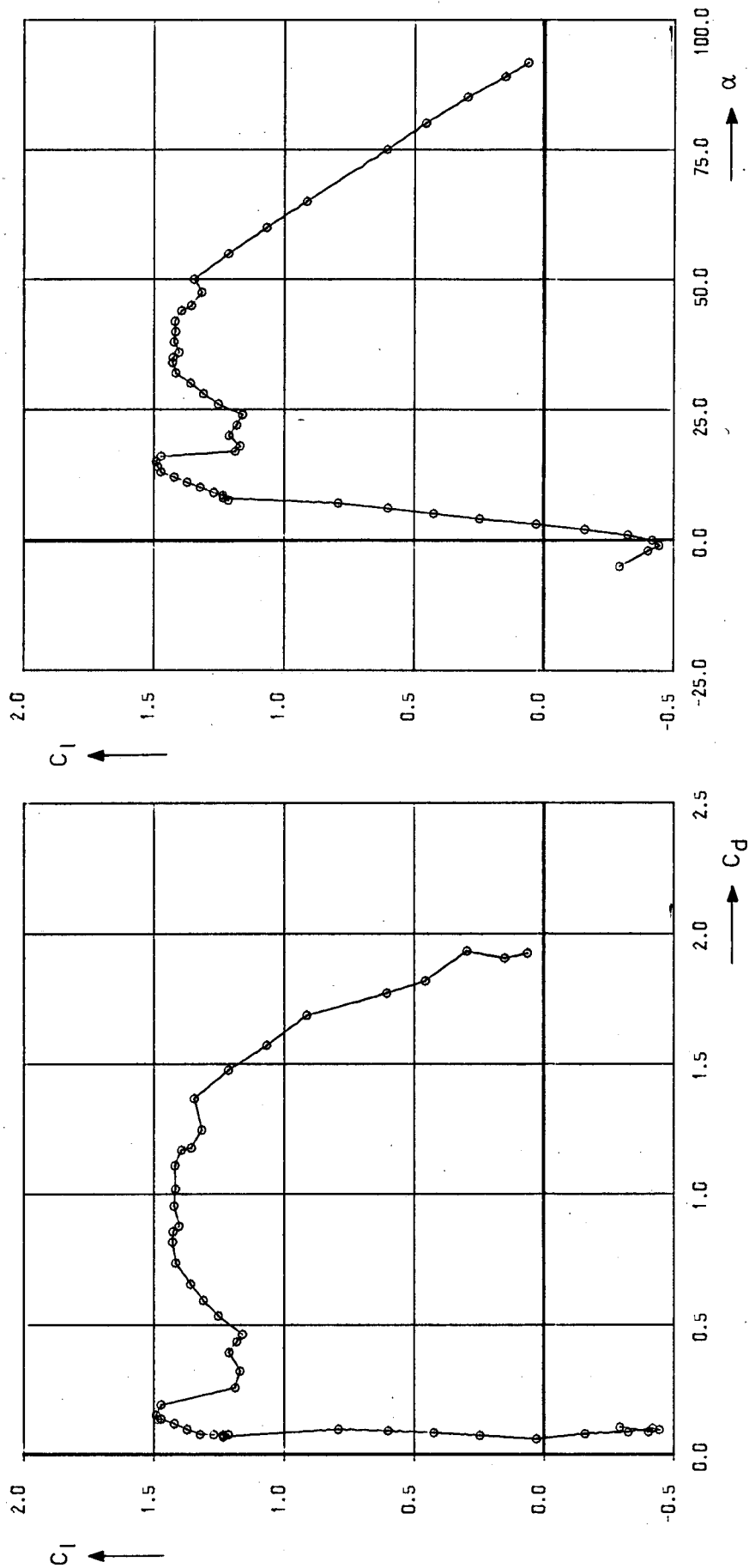


fig. 4 Section characteristics of curved plate.
Reynolds number: 60,000 , model code: - , -



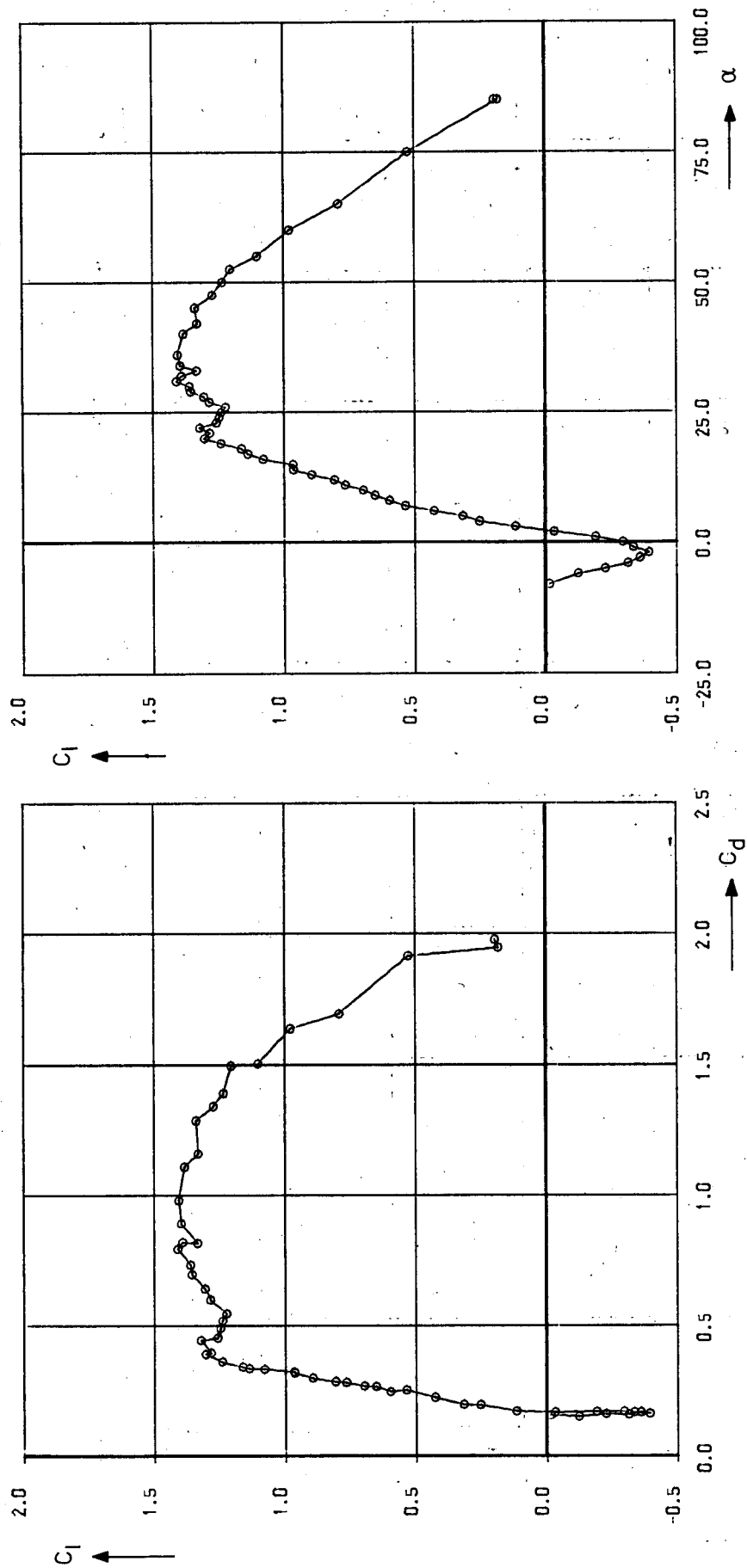


fig. 6 Section characteristics of curved plate.
 Reynolds number: 60.000 , model code: 25,-155

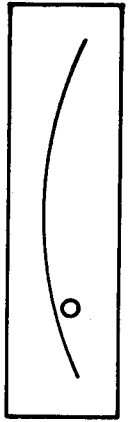
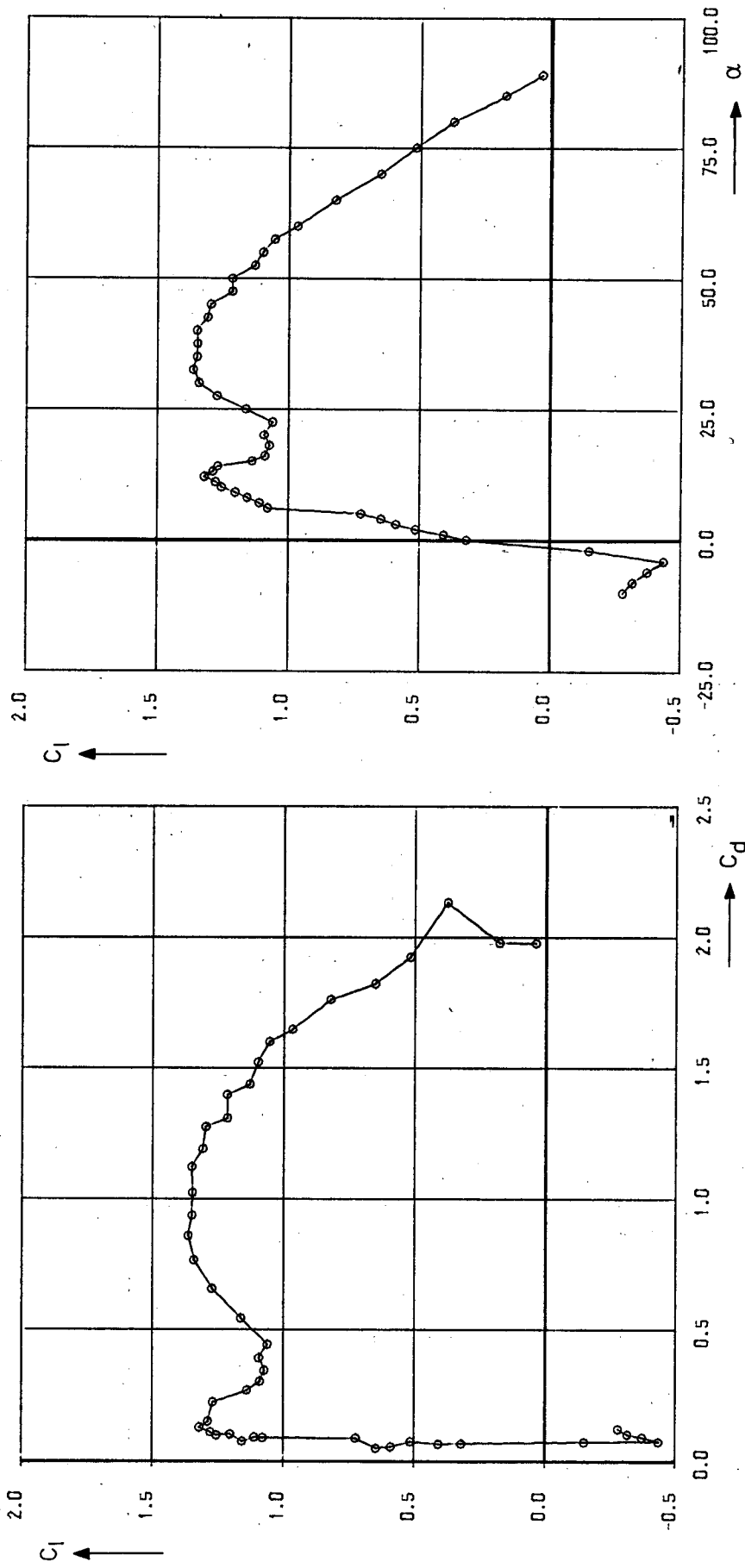


fig. 7 Section characteristics of curved plate.
Reynolds number: 60.000 , model code: 25,+ 1.55

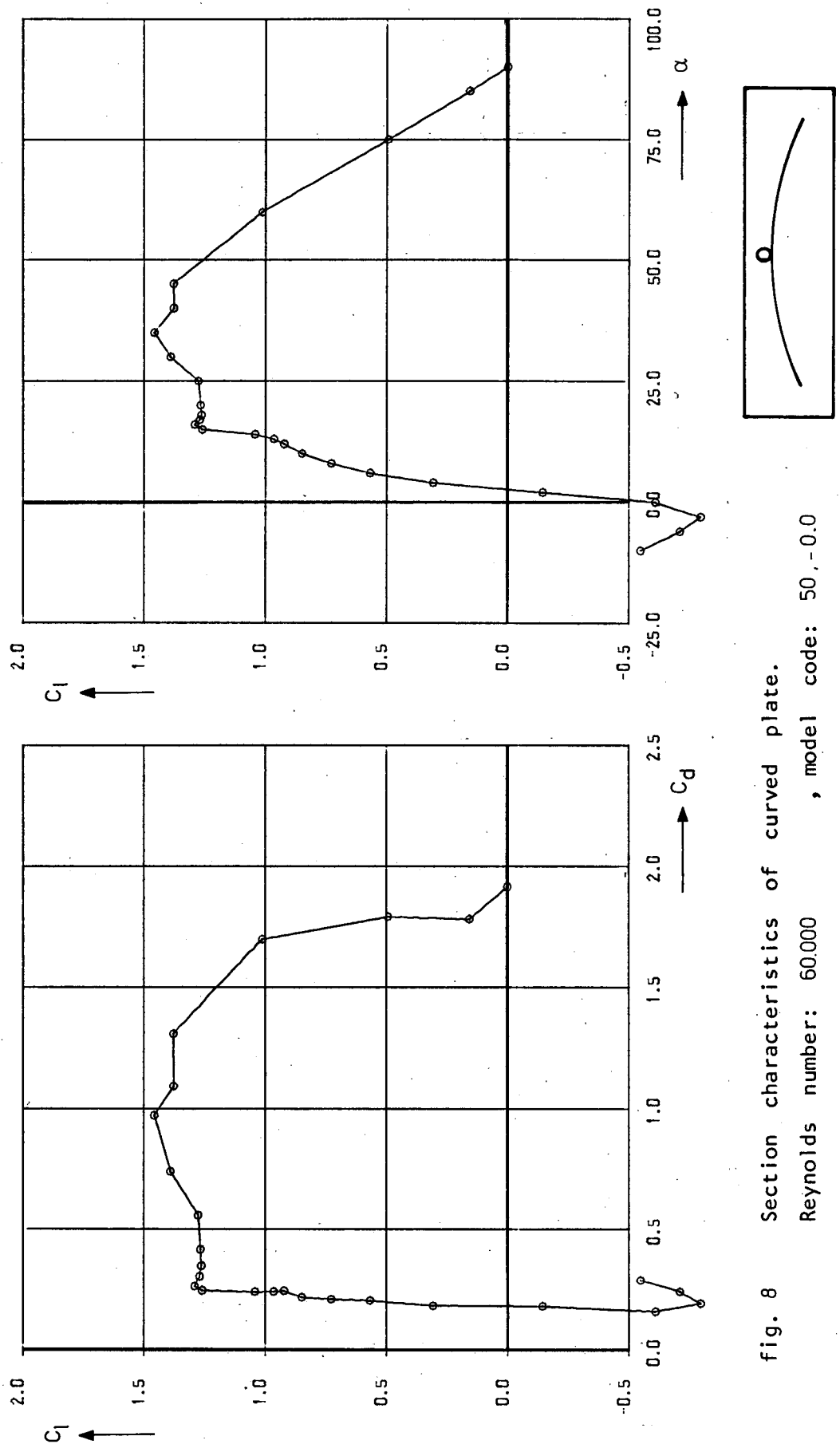


fig. 8 Section characteristics of curved plate.
Reynolds number: 60,000 , model code: 50,-0.0

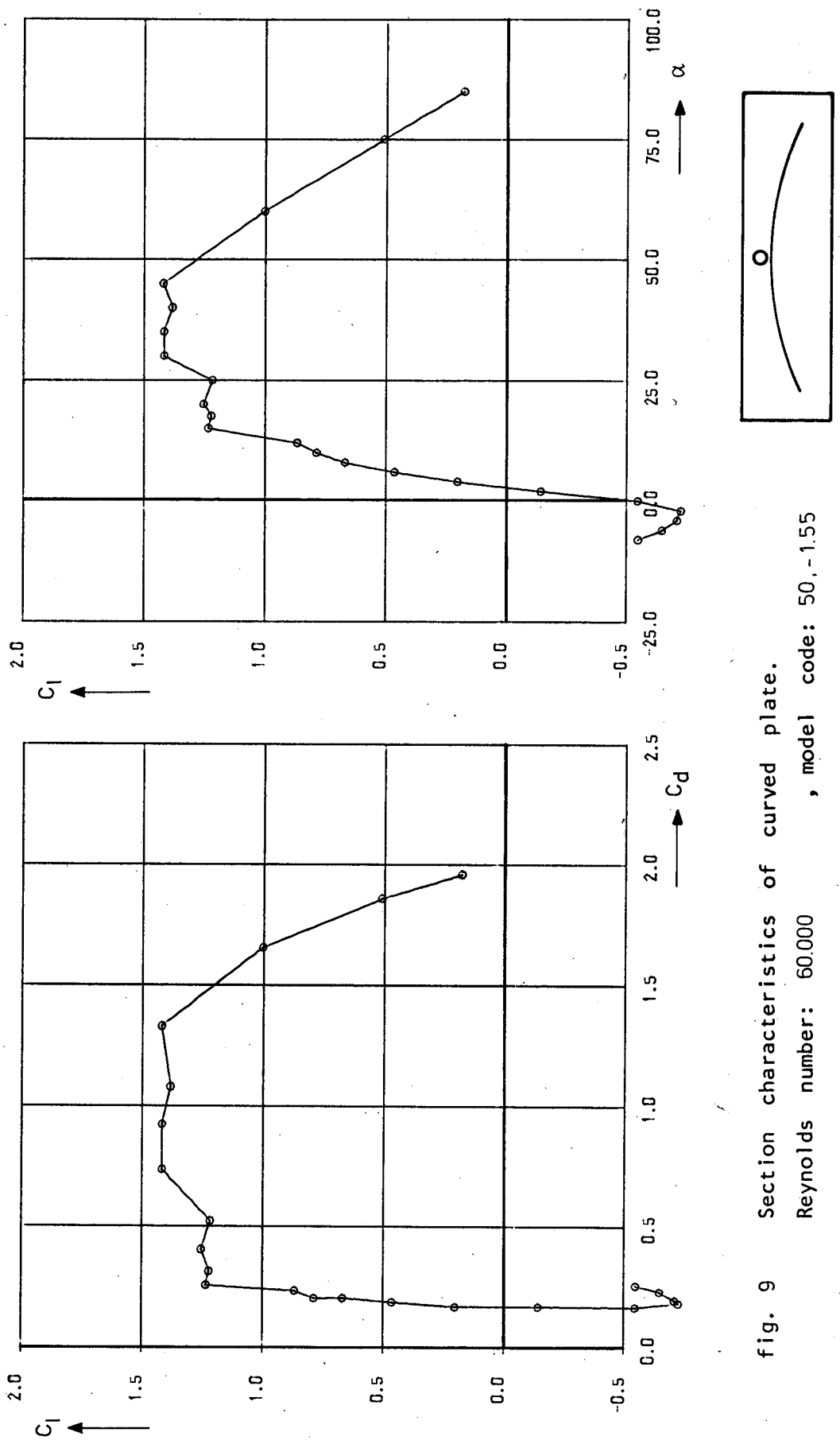


fig. 9 Section characteristics of curved plate.
Reynolds number: 60,000 , model code: 50,-1.55

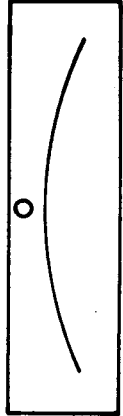
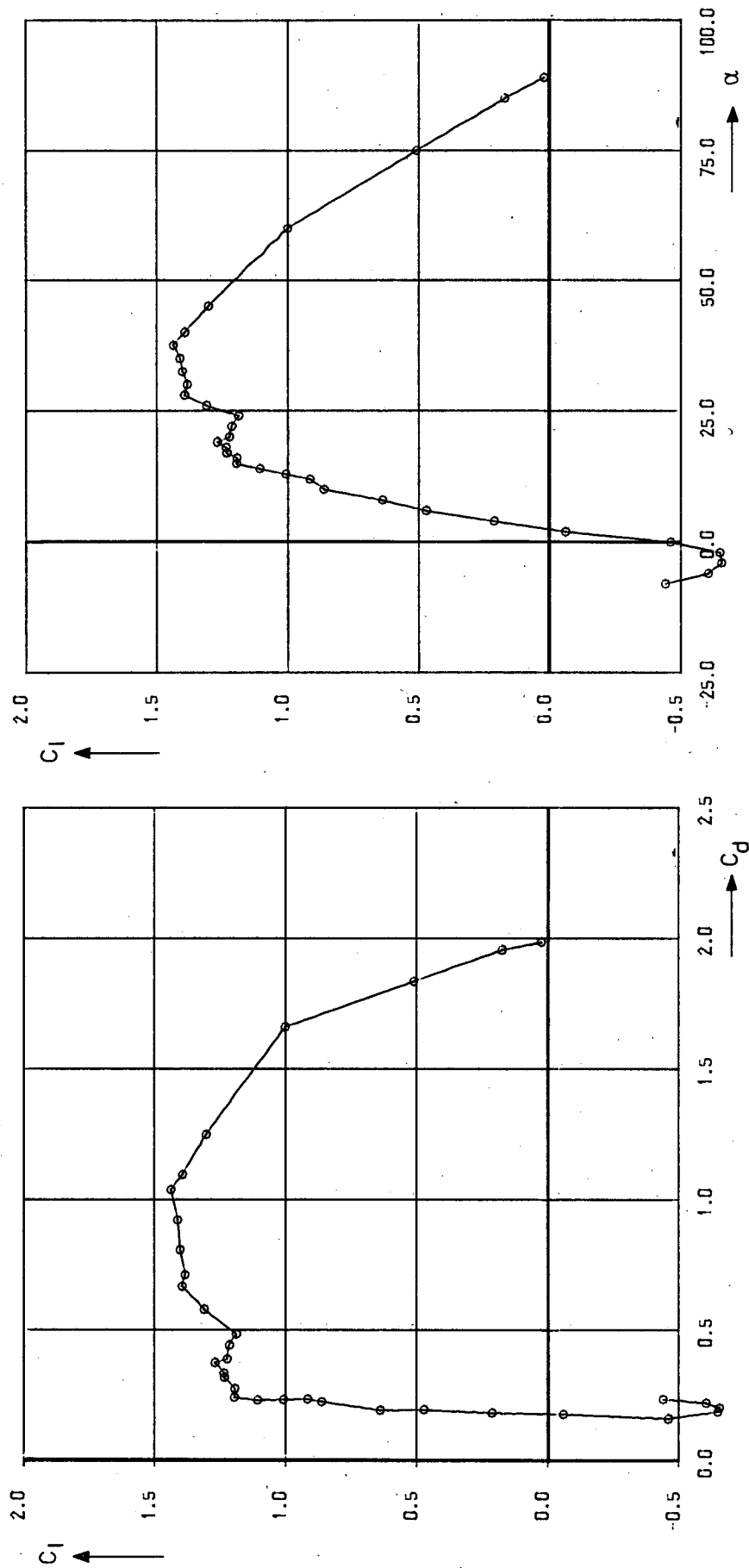


fig. 10 Section characteristics of curved plate.

Reynolds number: 60,000 , model code: 50,-4.0

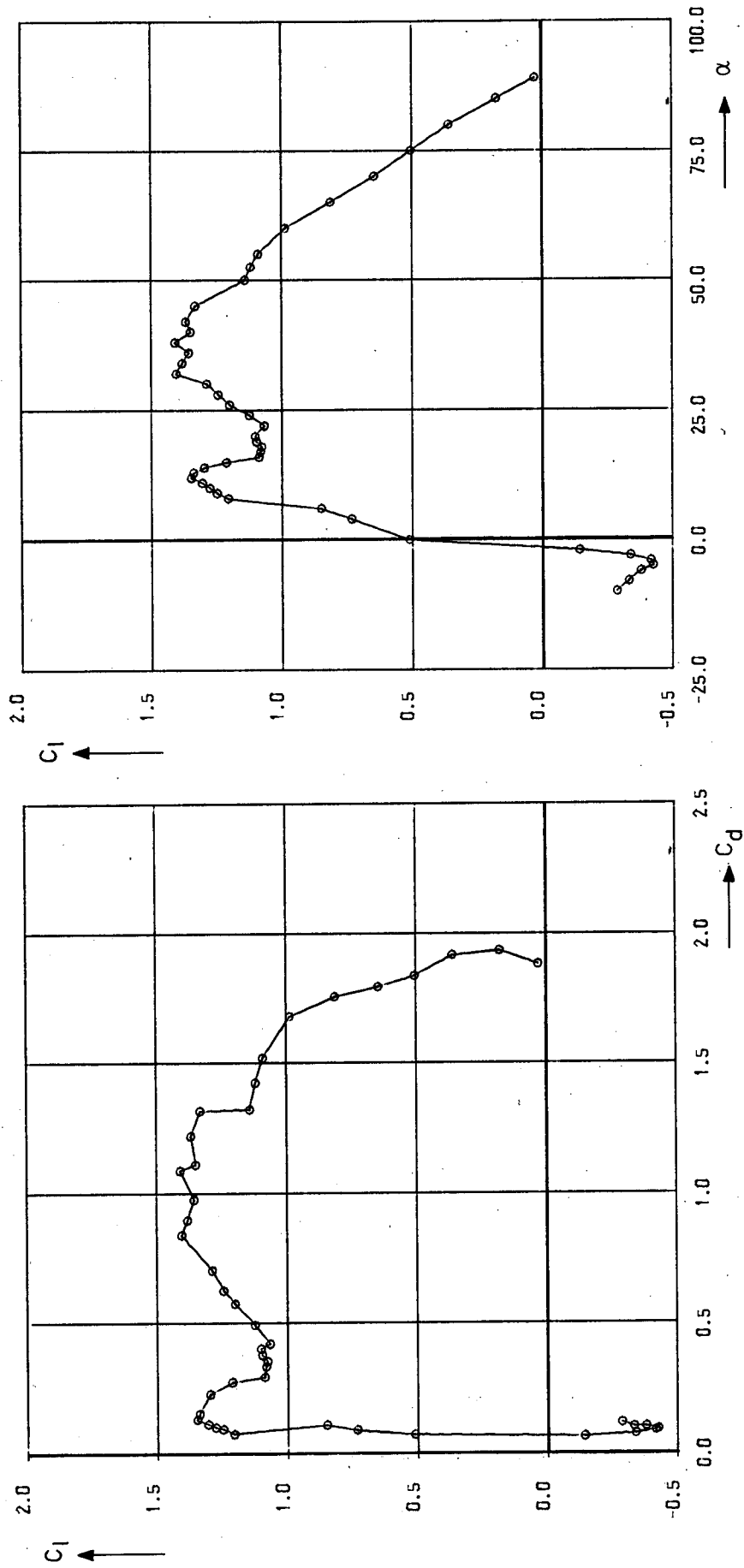


fig. 11 Section characteristics of curved plate.
Reynolds number: 60.000 , model code: 50, + 4.0

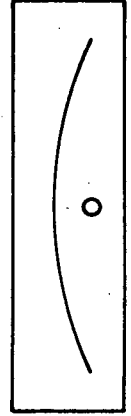
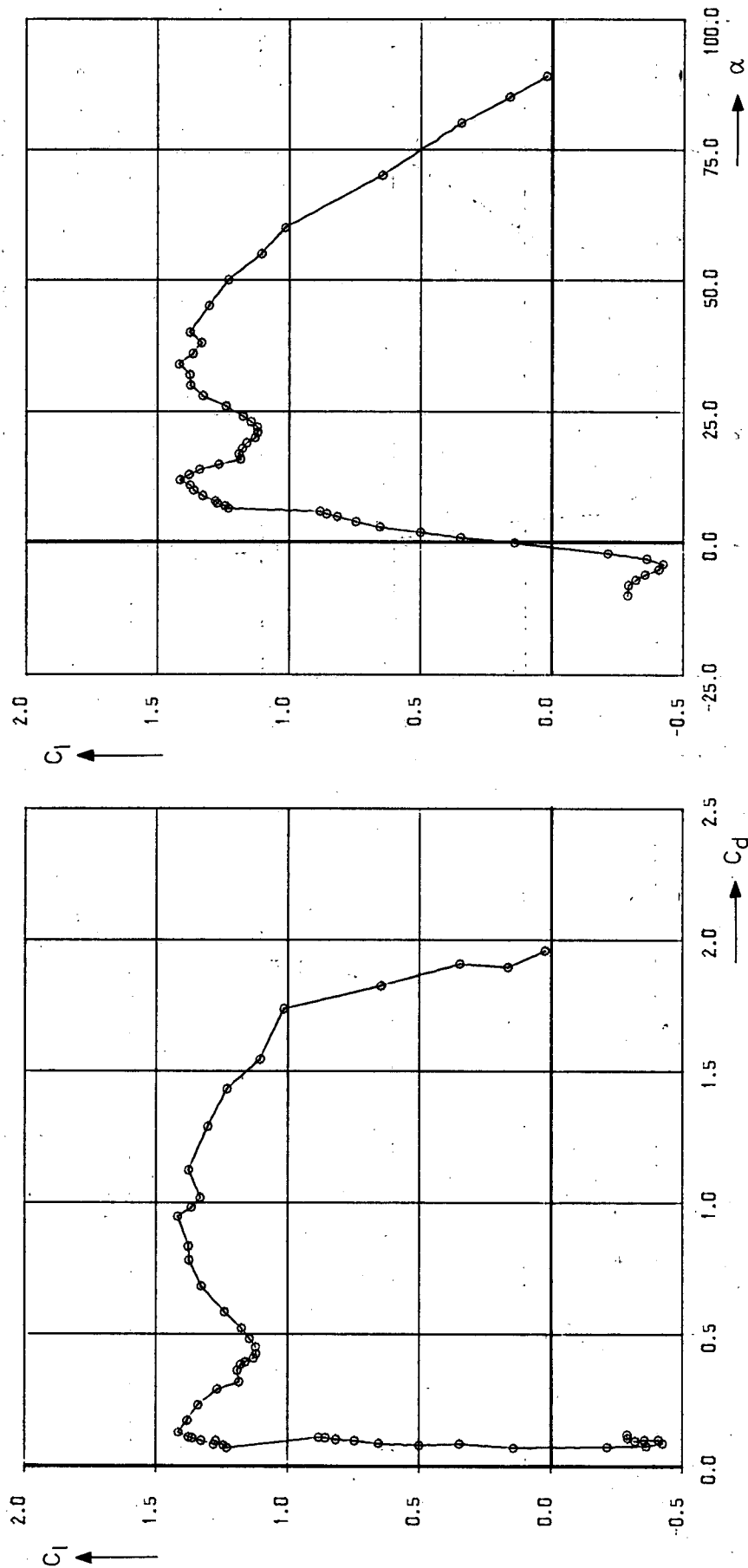


fig. 12 Section characteristics of curved plate.

Reynolds number: 60,000 , model code: 50,+8.0

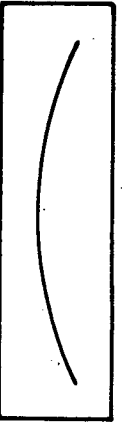
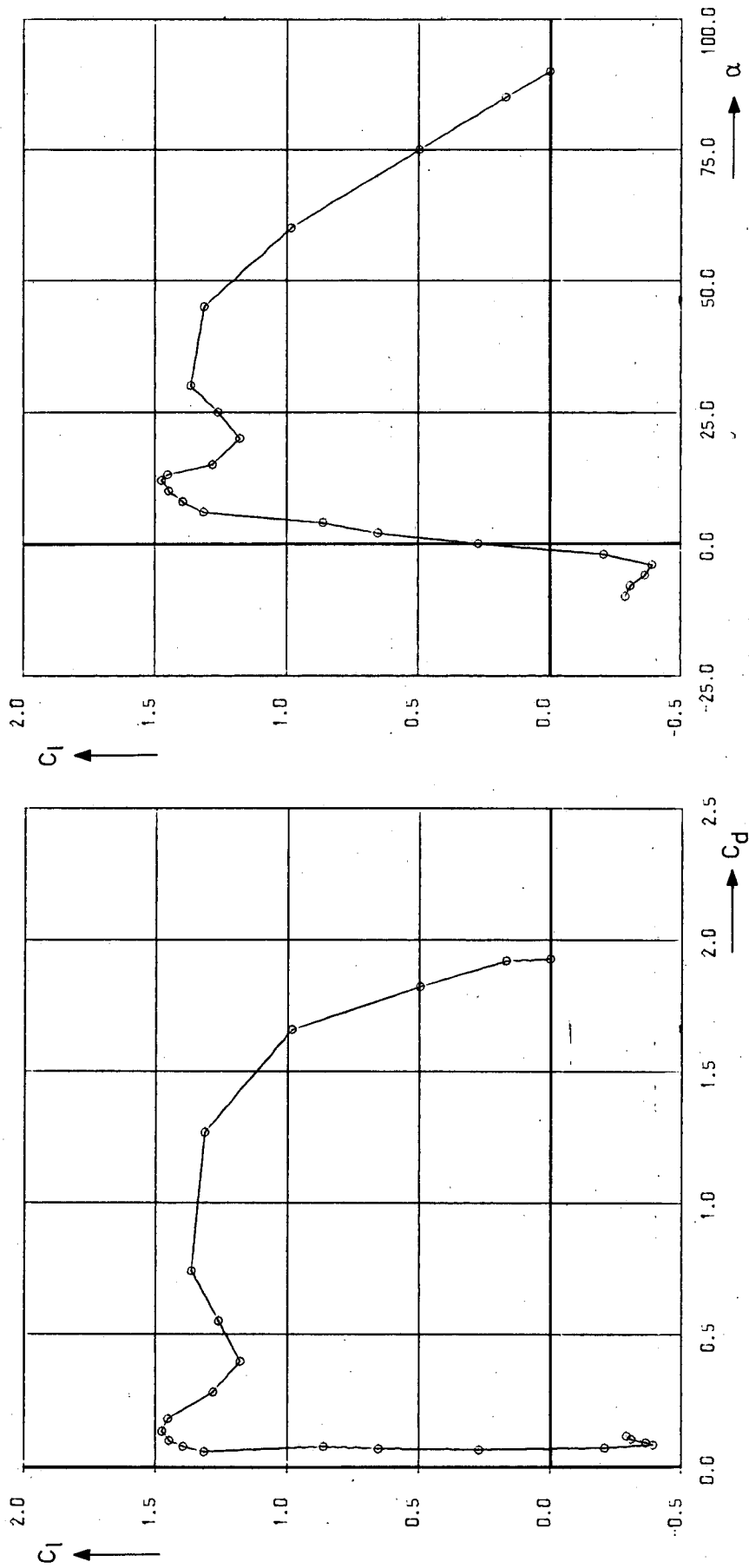


fig. 13 Section characteristics of curved plate.
 Reynolds number: 100,000 , model code: -.-

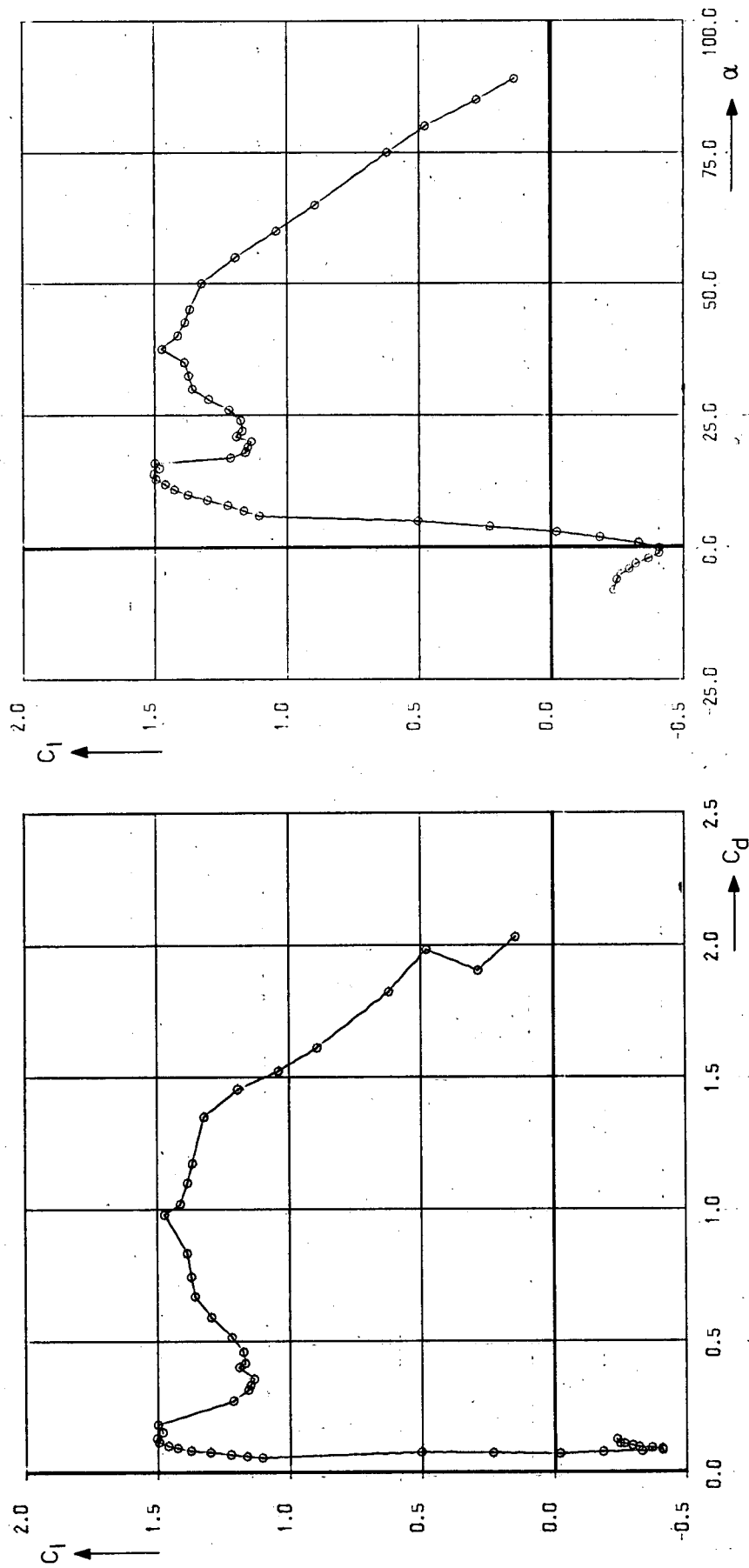


fig. 14 Section characteristics of curved plate.
 Reynolds number: 100.000 , model code: 0+0.0

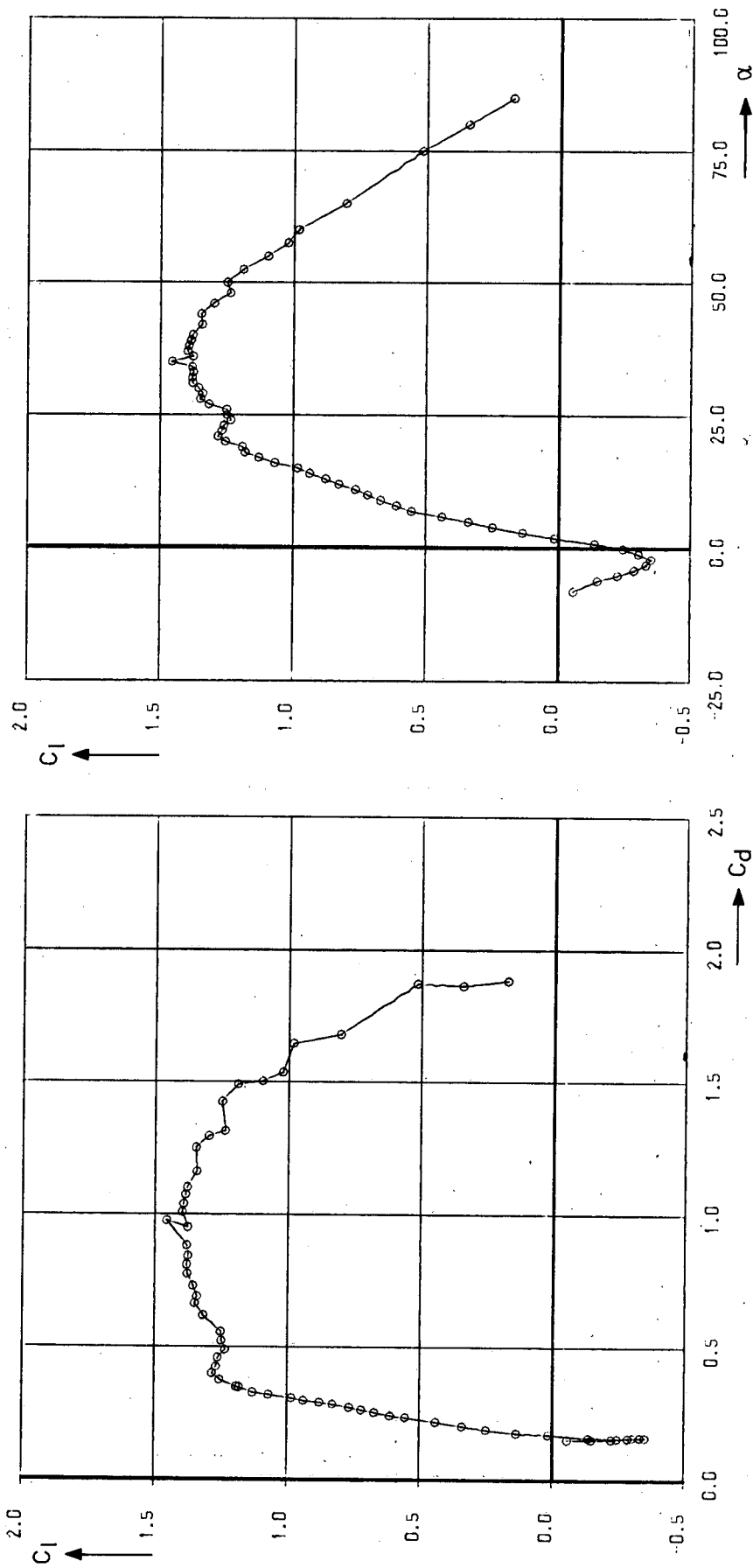


fig. 15 Section characteristics of curved plate.

Reynolds number: 100.000 , model code: 25,-1.55

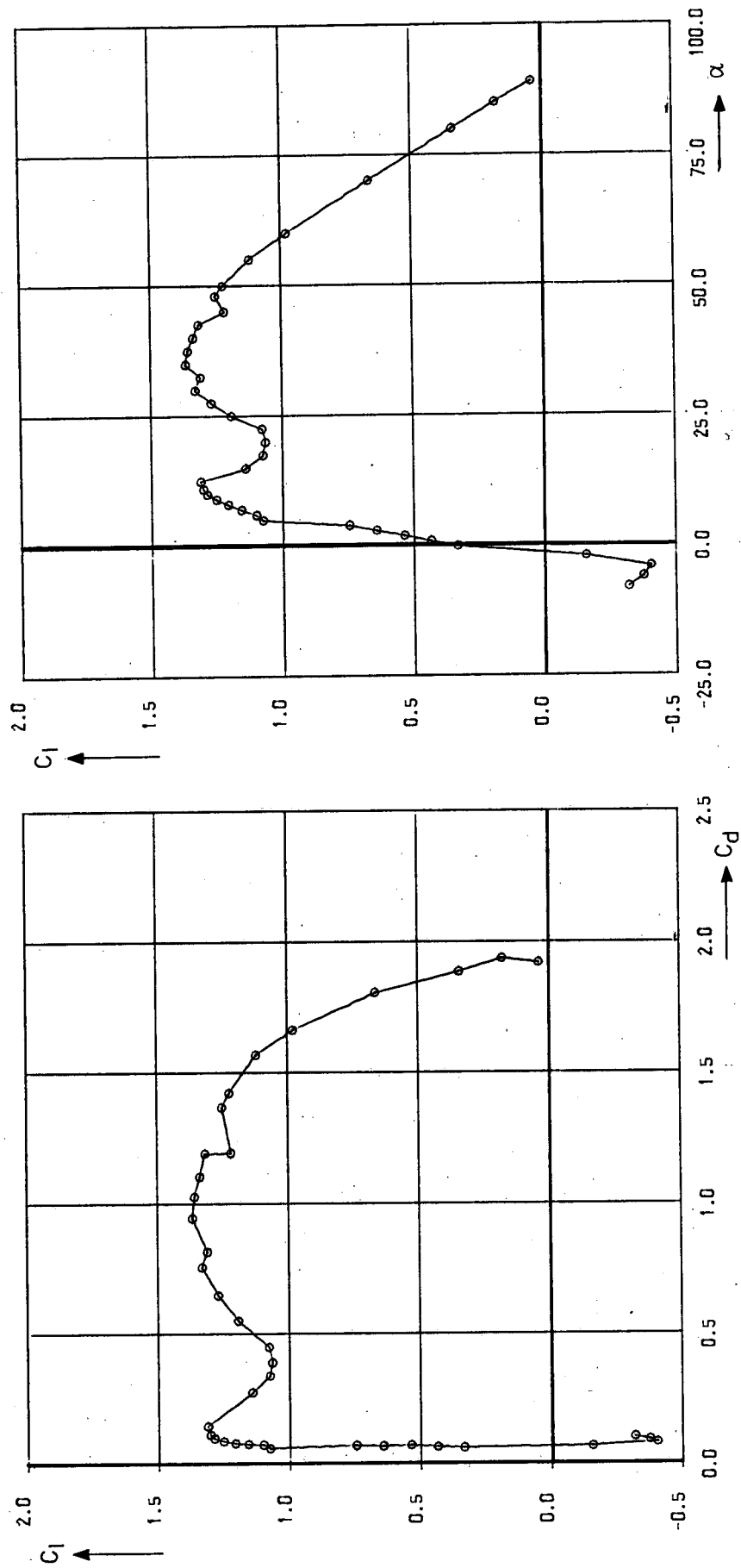


fig. 16 Section characteristics of curved plate.

Reynolds number: 100.000 , model code: 25,+1.55

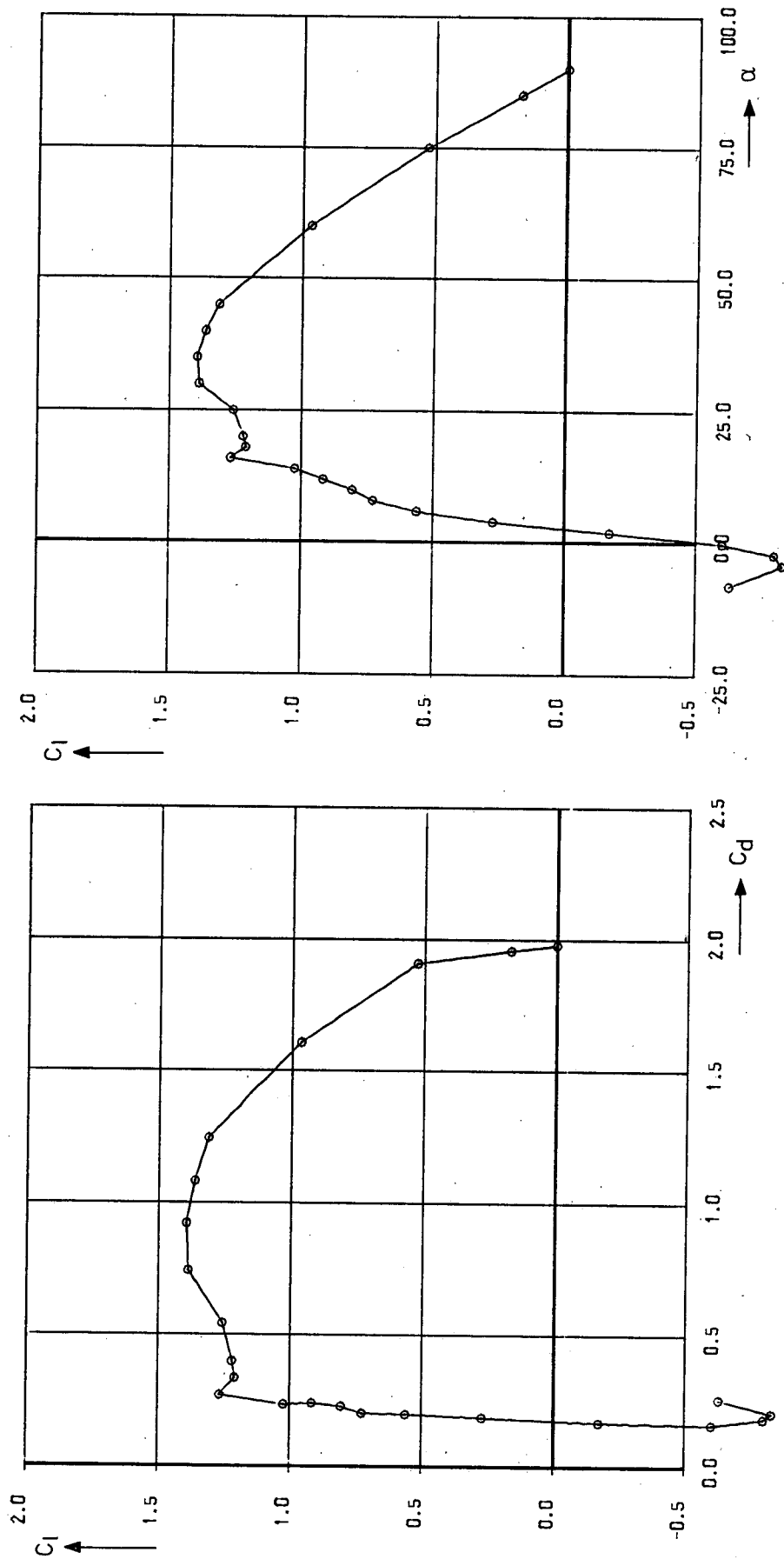


fig. 17 Section characteristics of curved plate.

Reynolds number: 100,000 , model code: 50,-0.0

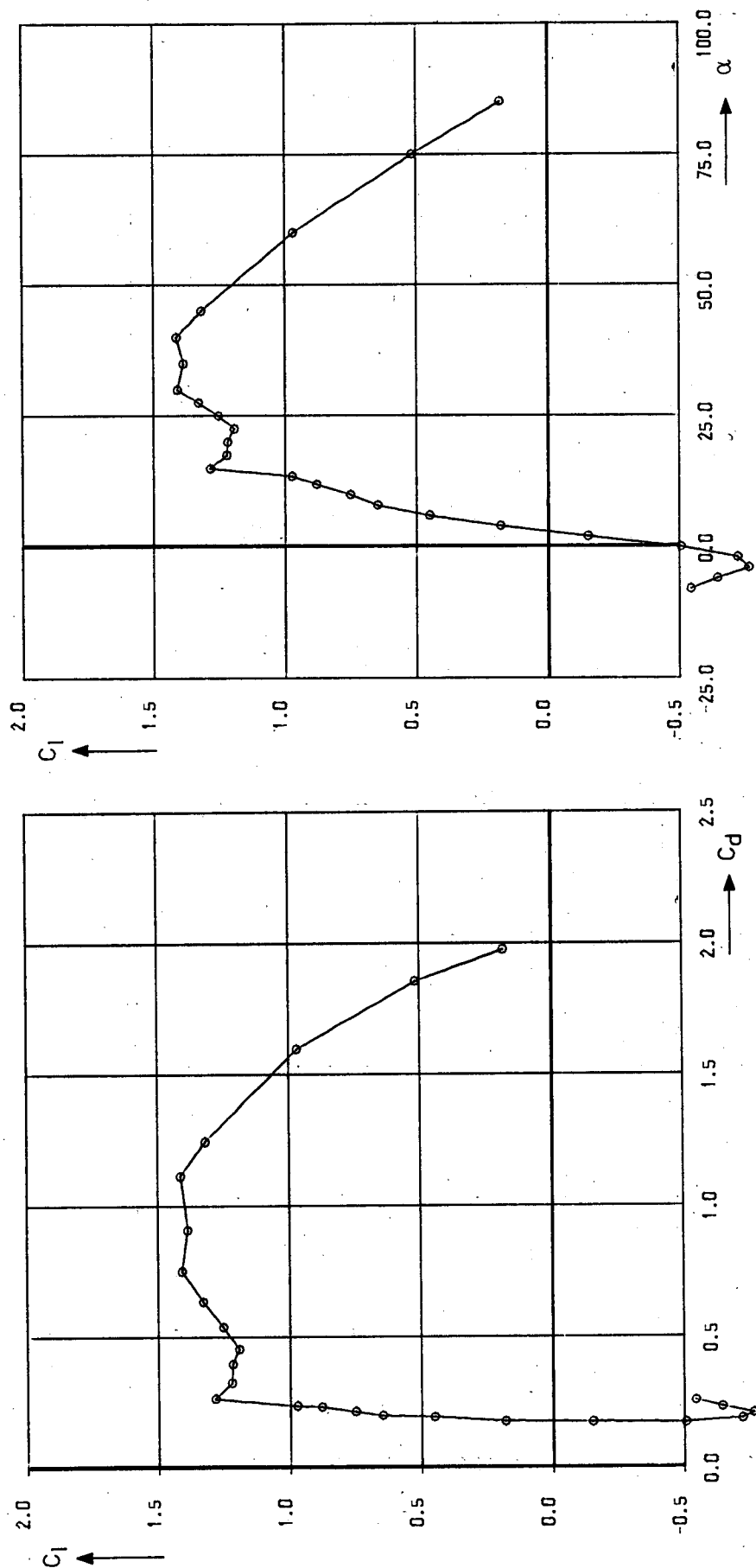


fig. 18 Section characteristics of curved plate.

Reynolds number: 100,000

, model code: 50,-1.55

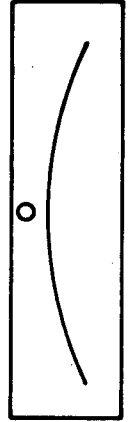
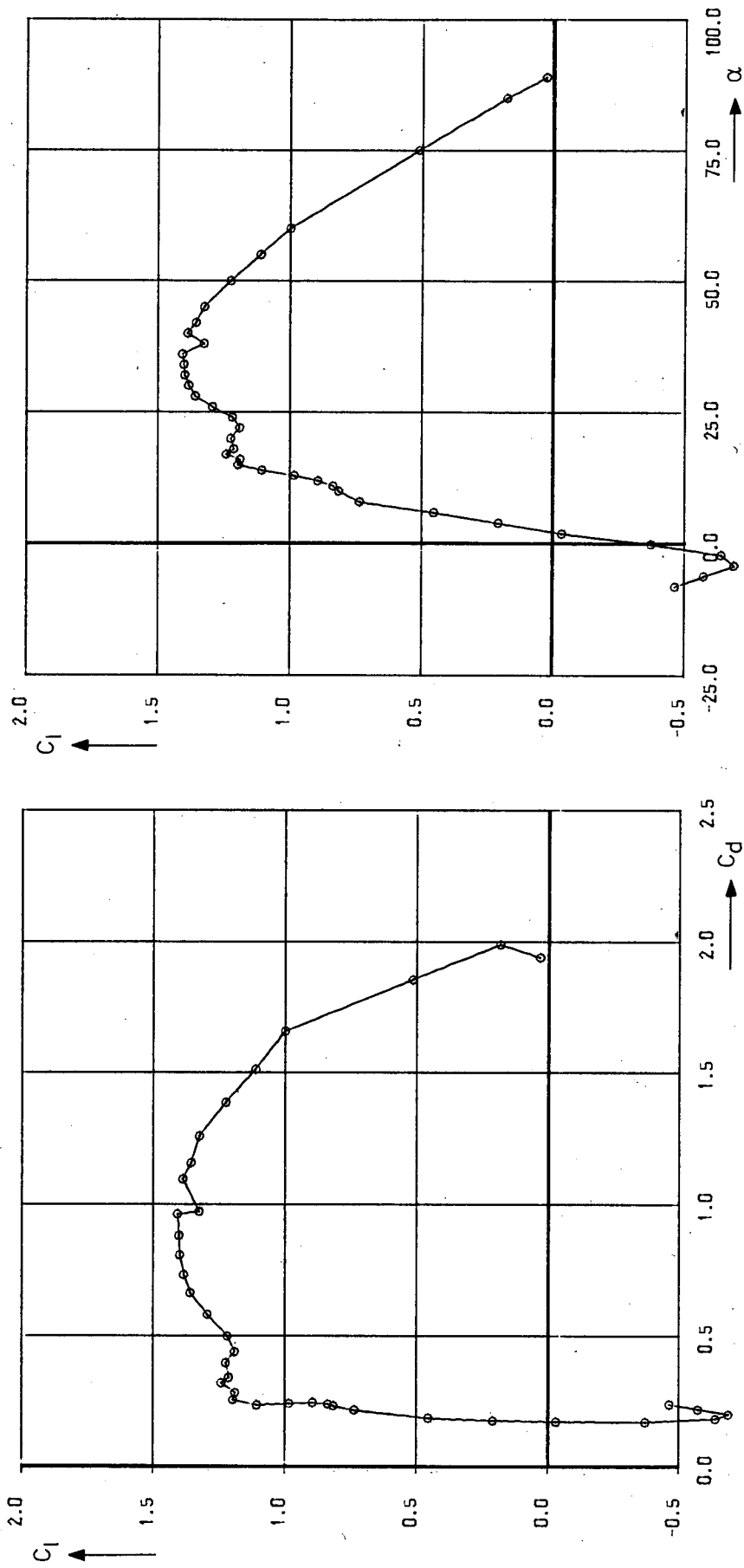


fig. 19 Section characteristics of curved plate.

Reynolds number: 100.000 , model code: 50,-4.0

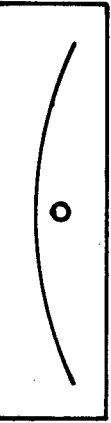
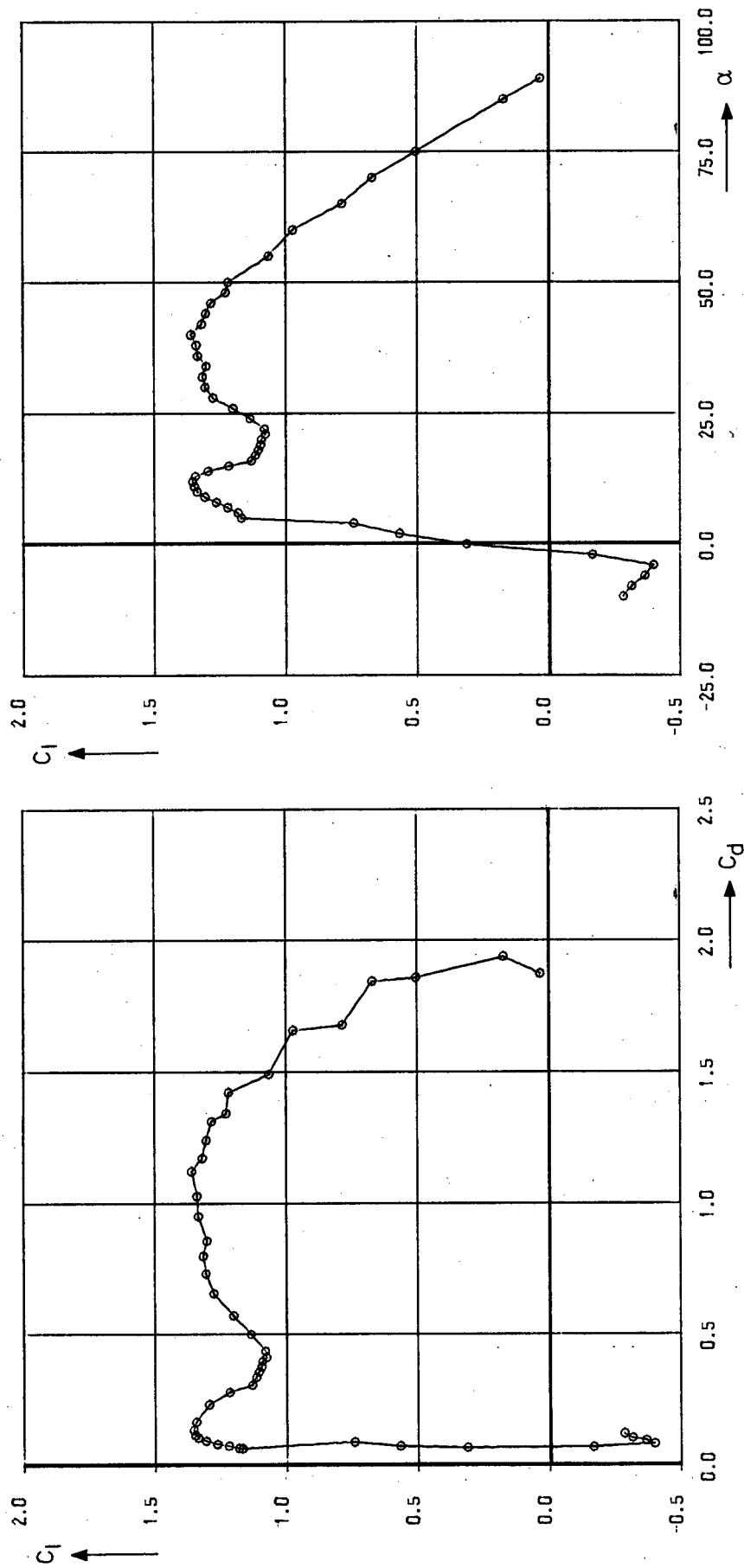


fig. 20 Section characteristics of curved plate.
Reynolds number: 100,000 , model code: 50,+4.0

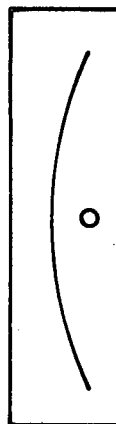
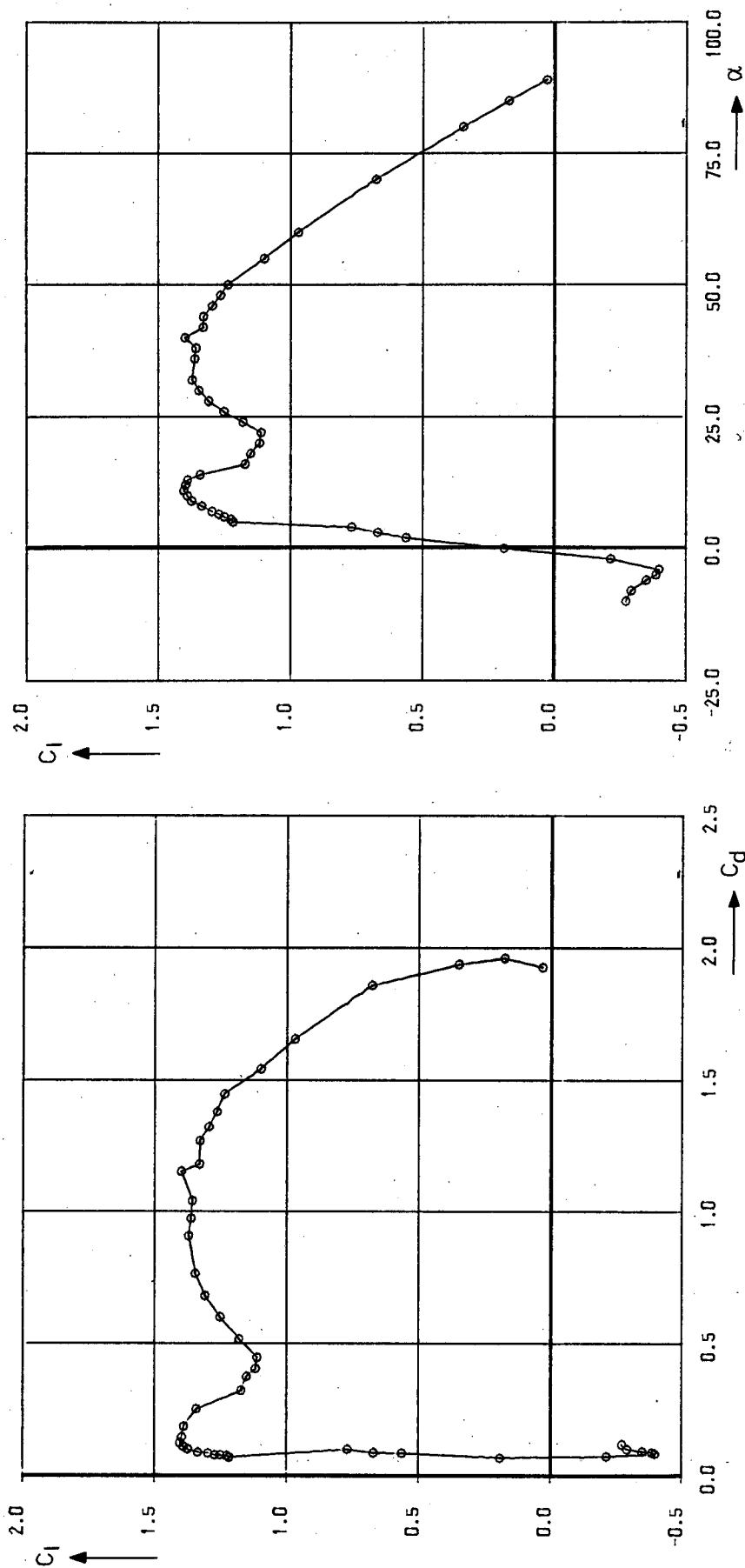


fig. 21 Section characteristics of curved plate.

Reynolds number: 100,000 , model code: 50,+8.0

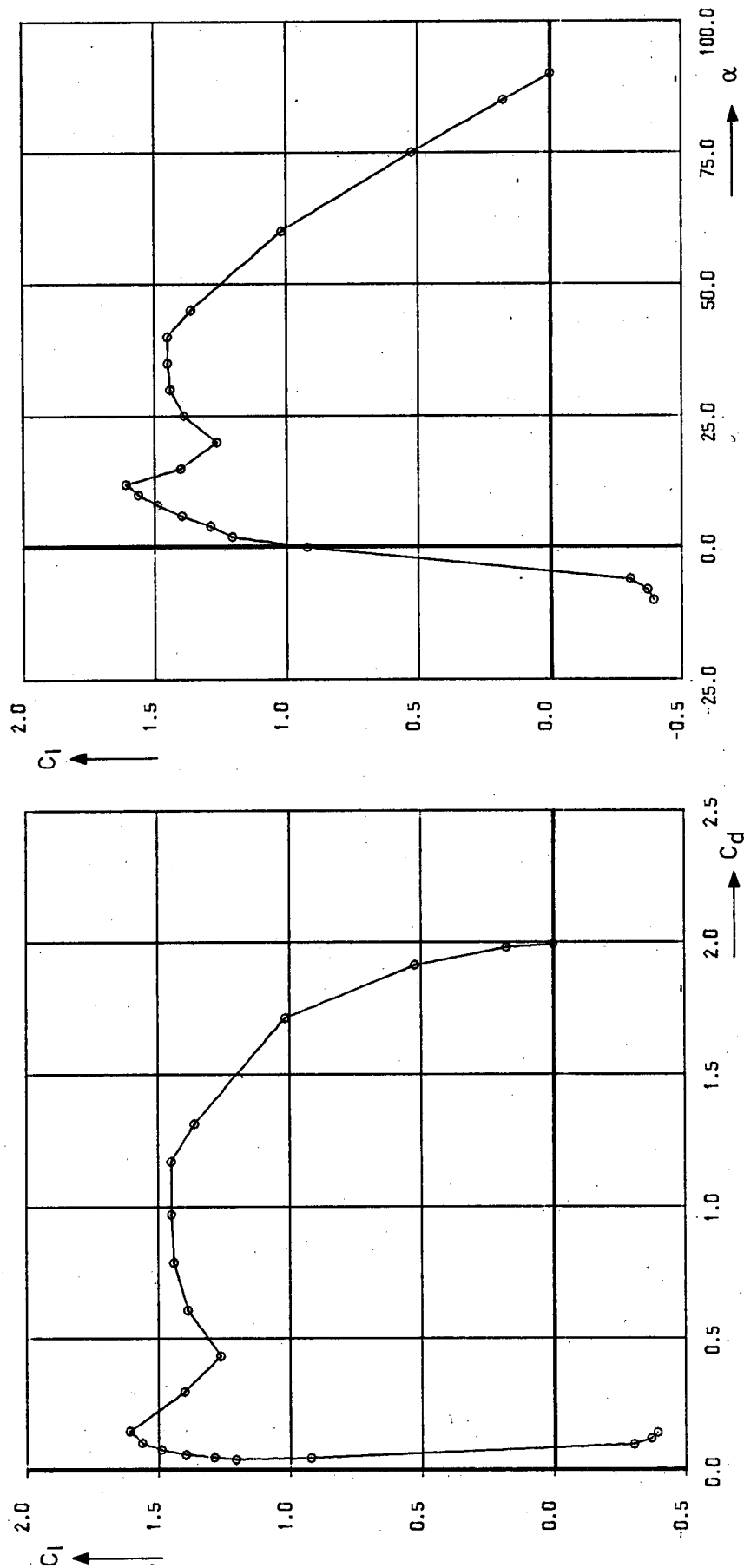


fig. 22 Section characteristics of curved plate.
 Reynolds number: 200,000 , model code: -.-

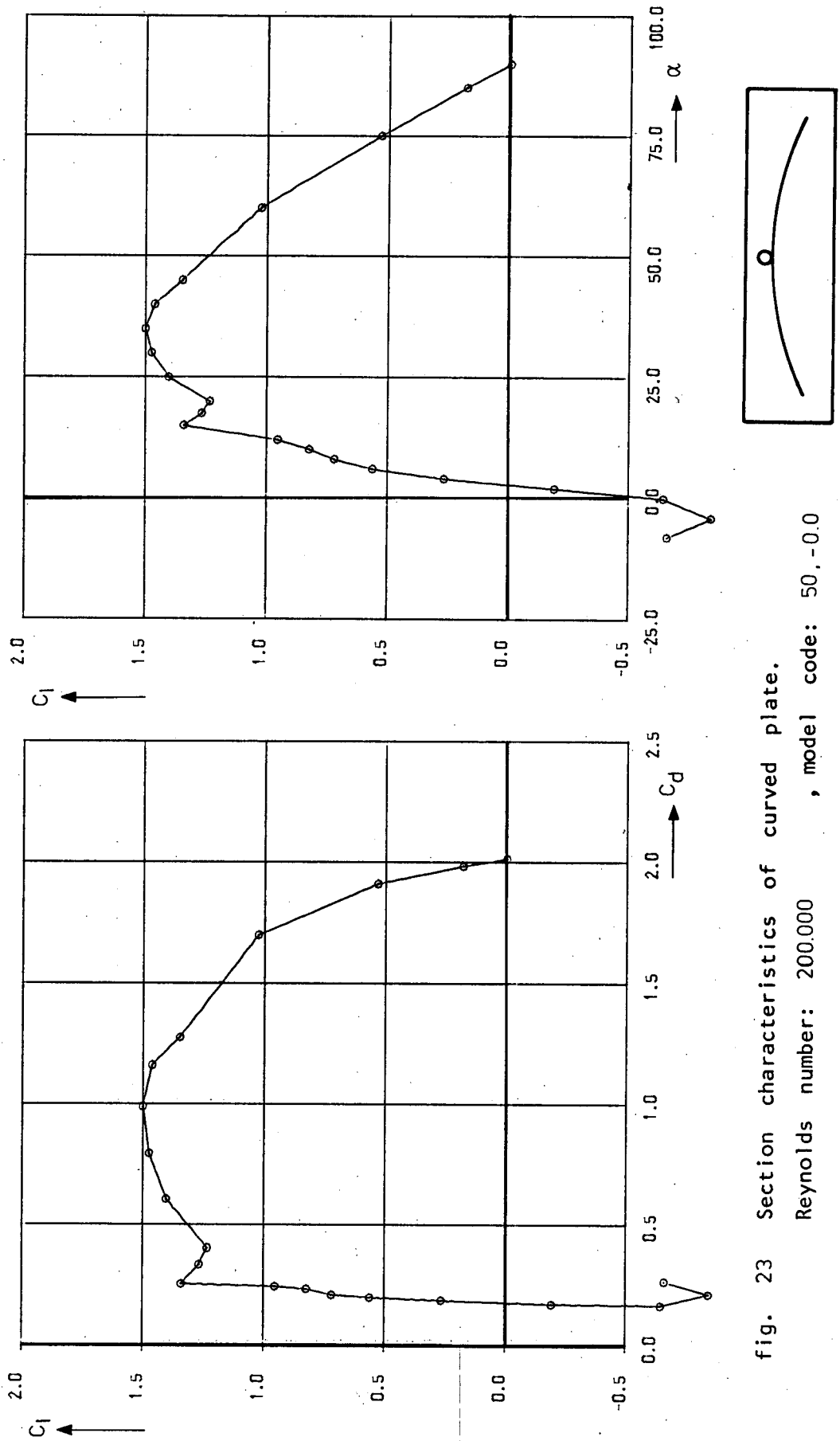


fig. 23 Section characteristics of curved plate.

Reynolds number: 200,000 , model code: 50,-0.0

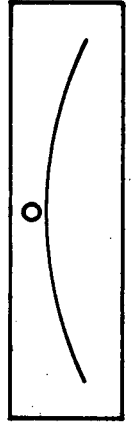
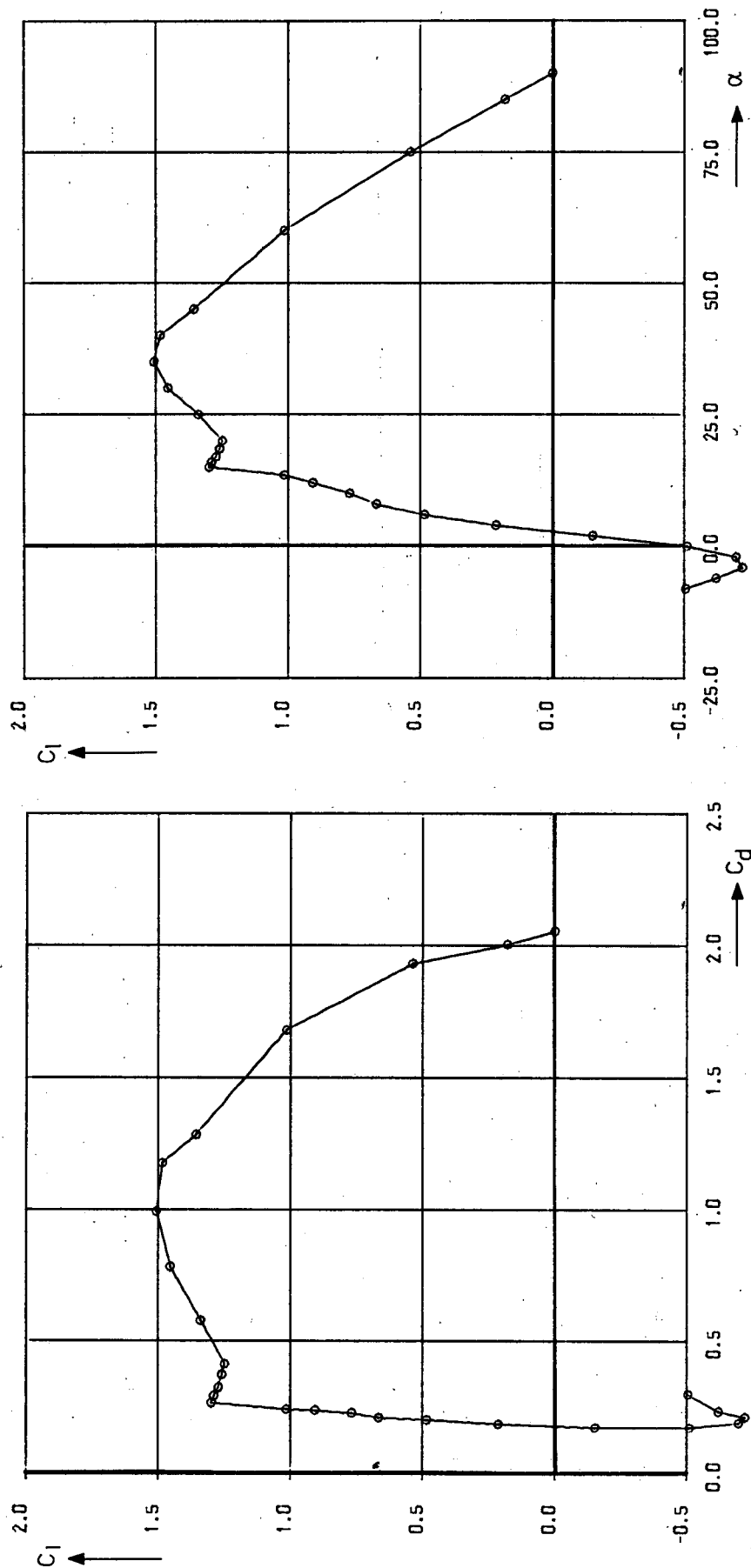


fig. 24 Section characteristics of curved plate.

Reynolds number: 200.000 , model code: 50.-155

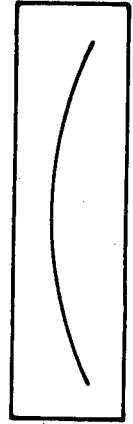
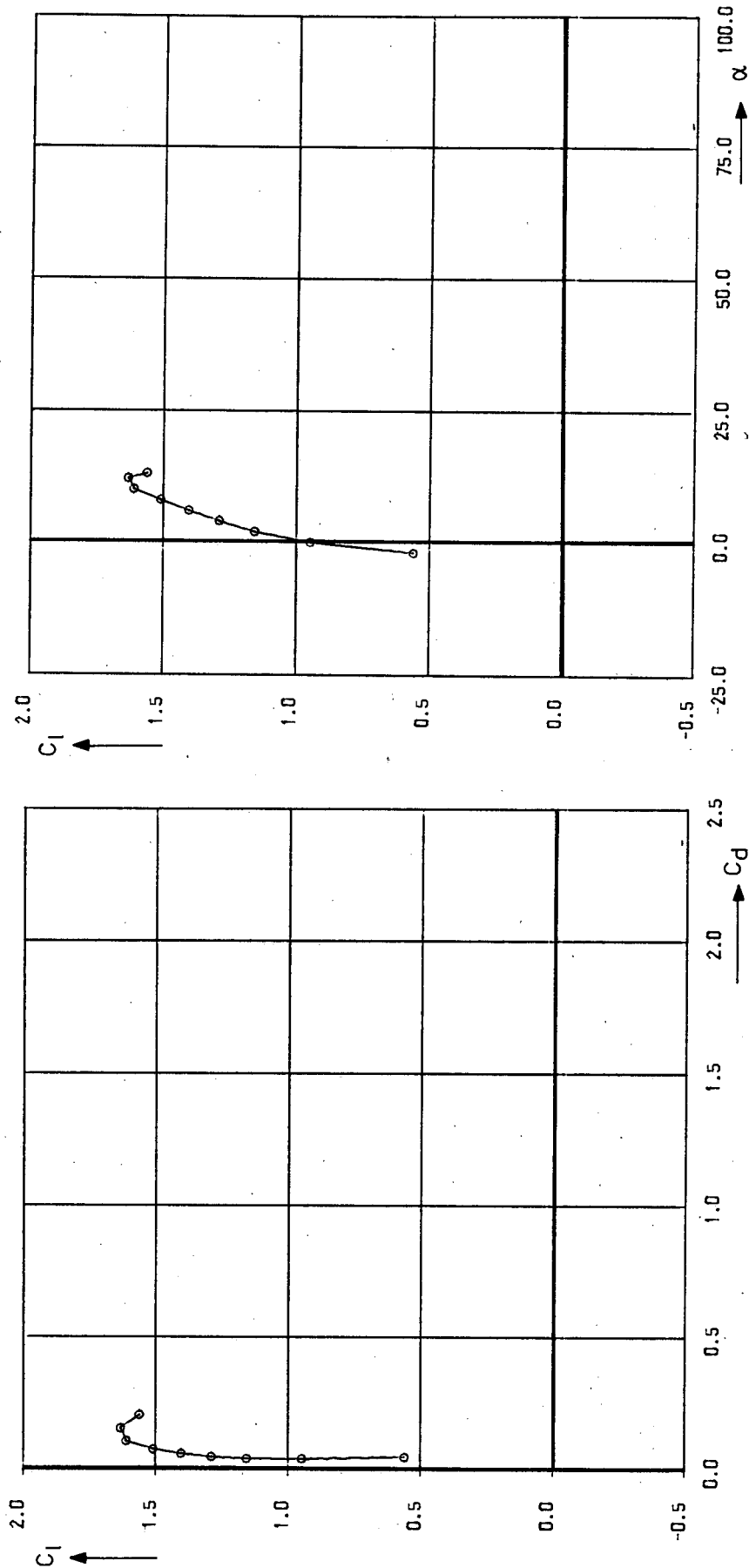


fig. 25 Section characteristics of curved plate.

Reynolds number: 350.000 , model code: -,-

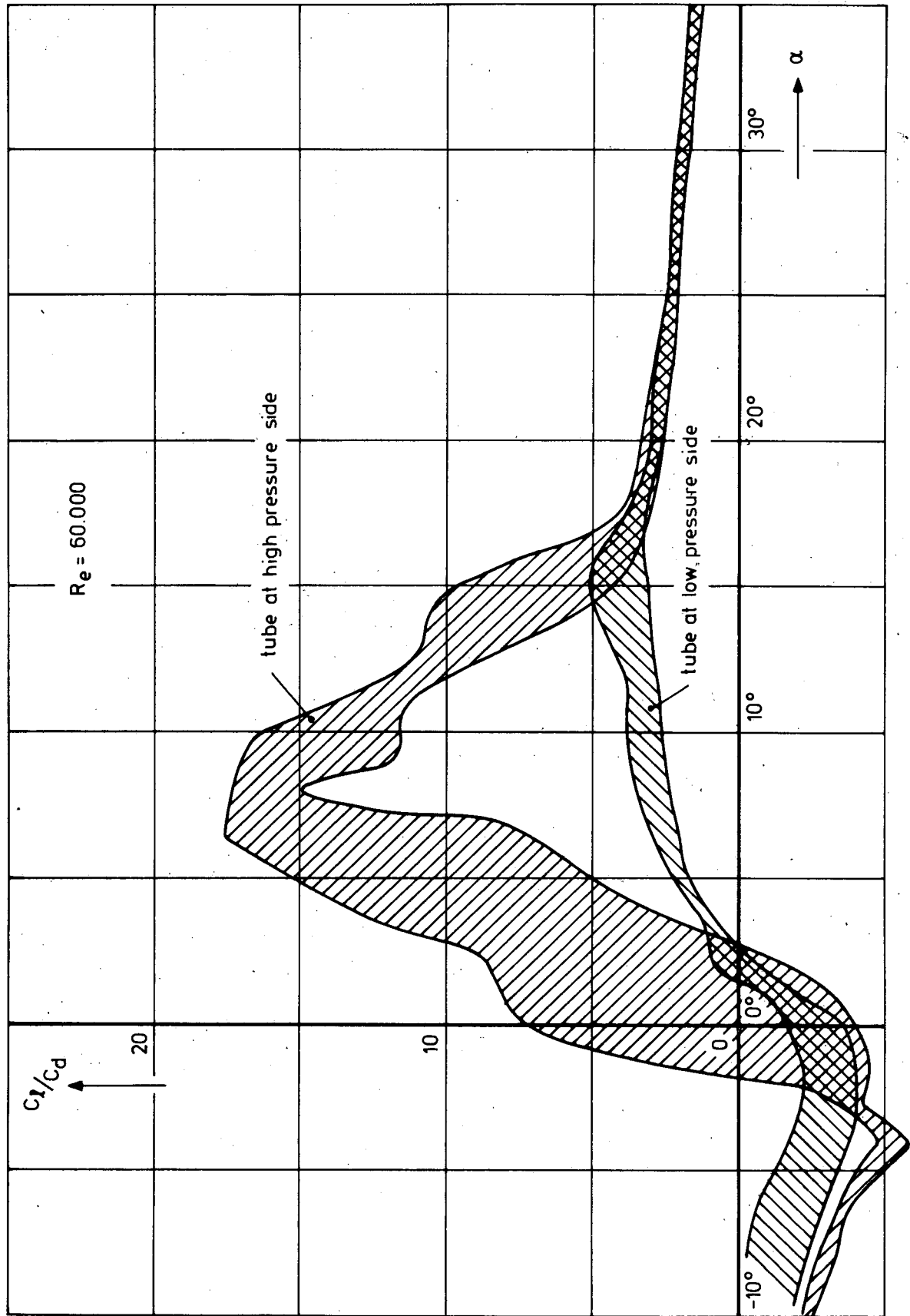


Fig. 26: Comparisons between tube positions at low- and high-pressure side of the blade.

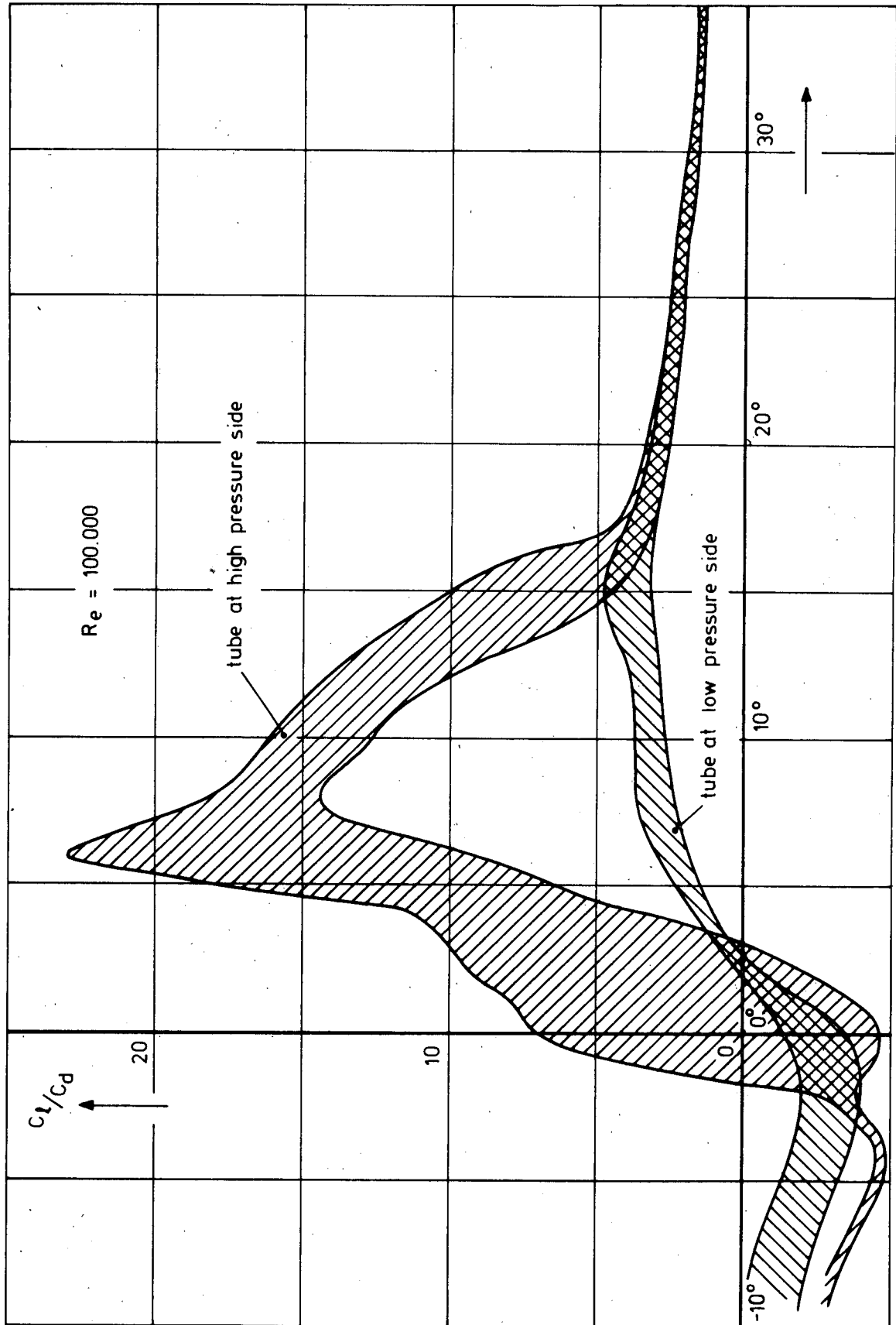


Fig. 27: Comparisons between tube positions at low- and high-pressure side of the blade.

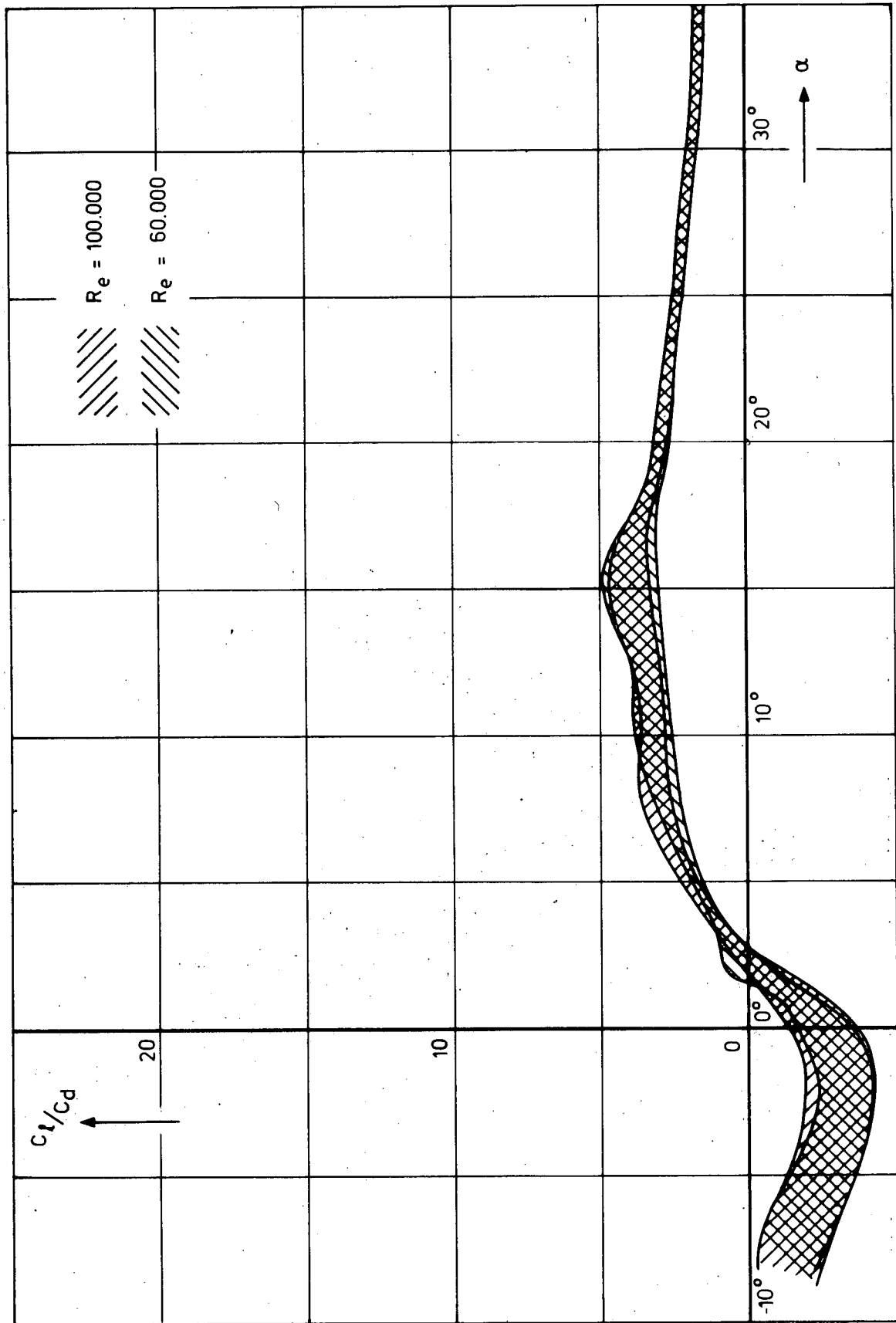


Fig. 28: Comparison between Reynolds numbers 60,000 and 100,000, tube at low pressure side of the blade.

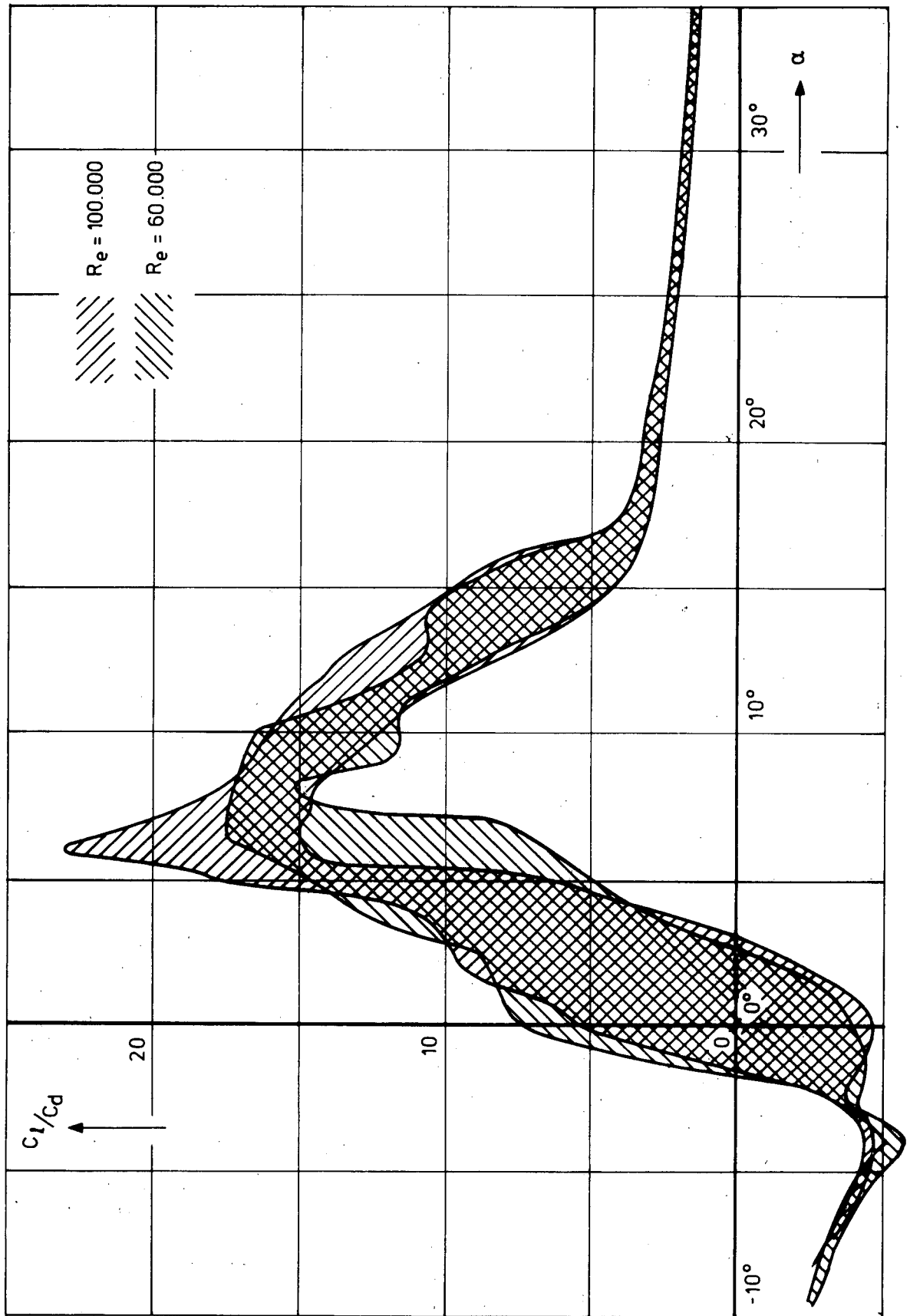


Fig. 29: Comparison between Reynoldsnumbers 60.000 and 100.000, tube at high pressure side of the blade.

